HALF-PLANE IMPEDANCE HELMHOLTZ PROBLEM

3.1 Introduction

In this chapter we study the perturbed half-plane impedance Helmholtz problem using integral equation techniques and the boundary element method.

We consider the problem of the Helmholtz equation in two dimensions on a compactly perturbed half-plane with an impedance boundary condition. The perturbed half-plane impedance Helmholtz problem is a wave scattering problem around the bounded perturbation, which is contained in the upper half-plane. In acoustic scattering the impedance boundary-value problem appears when we suppose that the normal velocity is proportional to the excess pressure on the boundary of the impenetrable perturbation or obstacle (vid. Section A.11). The special case of frequency zero for the volume waves has been treated already in Chapter II. The three-dimensional case is considered in Chapter V, whereas the full-plane impedance Helmholtz problem with a bounded impenetrable obstacle is treated thoroughly in Appendix C.

The main application of the problem corresponds to outdoor sound propagation, but it is also used to describe the propagation of radio waves above the ground and of water waves in shallow waters near the coast (harbor oscillations). The problem was at first considered by Sommerfeld (1909) to describe the long-distance propagation of electromagnetic waves above the earth. Different results for the electromagnetic problem were then obtained by Weyl (1919) and later again by Sommerfeld (1926). After the articles of Van der Pol & Niessen (1930), Wise (1931), and Van der Pol (1935), the most useful results up to that time were generated by Norton (1936, 1937). We can likewise mention the later works of Baños & Wesley (1953, 1954) and Baños (1966). The application of the problem to outdoor sound propagation was initiated by Rudnick (1947). Other approximate solutions to the problem were thereafter found by Lawhead & Rudnick (1951*a*,*b*) and Ingard (1951). Solutions containing surface-wave terms were obtained by Wenzel (1974) and Chien & Soroka (1975, 1980). Further references are listed in Nobile & Hayek (1985). Other articles that attempt to solve the problem are Briquet & Filippi (1977), Attenborough, Hayek & Lawther (1980), Filippi (1983), Li et al. (1994), and Attenborough (2002), and more recently also Habault (1999), Ochmann (2004), and Ochmann & Brick (2008), among others. For the two-dimensional case, in particular, we mention the articles of Chandler-Wilde & Hothersall (1995*a*,*b*) and Granat, Tahar & Ha-Duong (1999). The problem can be also found in the books of Greenberg (1971) and DeSanto (1992). The physical aspects of outdoor sound propagation can be found in Morse & Ingard (1961) and Embleton (1996). For the propagation of water waves in shallow waters near the coast (harbor oscillations) we cite the articles of Hsiao, Lin & Fang (2001) and Liu & Losada (2002), and the book of Mei, Stiassnie & Yue (2005).

The Helmholtz equation allows the propagation of volume waves inside the considered domain, and when it is supplied with an impedance boundary condition, then it allows also the propagation of surface waves along the boundary of the perturbed half-plane. The main difficulty in the numerical treatment and resolution of our problem is the fact that the

exterior domain is unbounded. We solve it therefore with integral equation techniques and a boundary element method, which require the knowledge of the associated Green's function. This Green's function is computed using a Fourier transform and taking into account the limiting absorption principle, following Durán, Muga & Nédélec (2005*a*, 2006) and Durán, Hein & Nédélec (2007*a*,*b*), but here an explicit expression is found for it in terms of a finite combination of elementary functions, special functions, and their primitives.

This chapter is structured in 13 sections, including this introduction. The direct scattering problem of the Helmholtz equation in a two-dimensional compactly perturbed half-plane with an impedance boundary condition is presented in Section 3.2. The computation of the Green's function, its far field, and its numerical evaluation are developed respectively in Sections 3.3, 3.4, and 3.5. The use of integral equation techniques to solve the direct scattering problem is discussed in Section 3.6. These techniques allow also to represent the far field of the solution, as shown in Section 3.7. The appropriate function spaces and some existence and uniqueness results for the solution of the problem are presented in Section 3.8. The dissipative problem is studied in Section 3.9. By means of the variational formulation developed in Section 3.10, the obtained integral equation is discretized using the boundary element method, which is described in Section 3.11. The boundary element calculations required to build the matrix of the linear system resulting from the numerical discretization are explained in Section 3.12. Finally, in Section 3.13 a benchmark problem based on an exterior half-circle problem is solved numerically.

3.2 Direct scattering problem

3.2.1 Problem definition

We consider the direct scattering problem of linear time-harmonic acoustic waves on a perturbed half-plane $\Omega_e \subset \mathbb{R}^2_+$, where $\mathbb{R}^2_+ = \{(x_1, x_2) \in \mathbb{R}^2 : x_2 > 0\}$, where the incident field u_I and the reflected field u_R are known, and where the time convention $e^{-i\omega t}$ is taken. The goal is to find the scattered field u as a solution to the Helmholtz equation in the exterior open and connected domain Ω_e, satisfying an outgoing radiation condition, and such that the total field u_T, decomposed as $u_T = u_I + u_R + u$, satisfies a homogeneous impedance boundary condition on the regular boundary $\Gamma = \Gamma_p \cup \Gamma_\infty$ (e.g., of class C^2). The exterior domain Ω_e is composed by the half-plane $\mathbb{R}^2_+$ with a compact perturbation near the origin that is contained in $\mathbb{R}^2_+$, as shown in Figure 3.1. The perturbed boundary is denoted by Γ_p, while Γ_∞ denotes the remaining unperturbed boundary of $\mathbb{R}^2_+$, which extends towards infinity on both sides. The unit normal $\boldsymbol{n}$ is taken outwardly oriented of Ω_e and the complementary domain is denoted by $\Omega_c = \mathbb{R}^2 \setminus \overline{\Omega_e}$. A given wave number $k > 0$ is considered, which depends on the pulsation ω and the speed of wave propagation c through the ratio $k = \omega/c$.

The total field u_T satisfies thus the Helmholtz equation

$$\Delta u_T + k^2 u_T = 0 \qquad \text{in } \Omega_e, \tag{3.1}$$

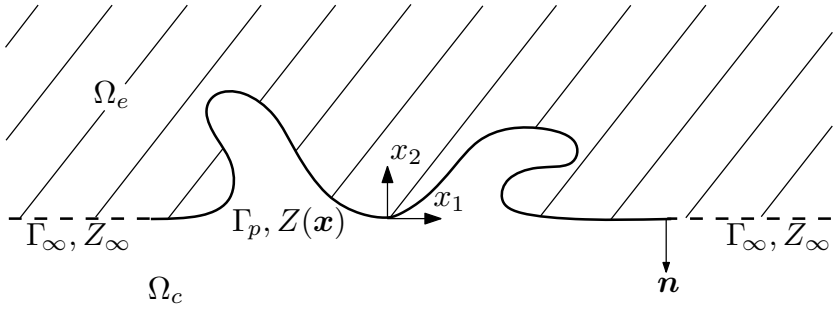

FIGURE 3.1. Perturbed half-plane impedance Helmholtz problem domain.

which is also satisfied by the incident field u_I, the reflected field u_R, and the scattered field u, due linearity. For the total field u_T we take the homogeneous impedance boundary condition

$$-\frac{\partial u_T}{\partial n} + Z u_T = 0 \qquad \text{on } \Gamma, \tag{3.2}$$

where Z is the impedance on the boundary, which is decomposed as

$$Z(\boldsymbol{x}) = Z_\infty + Z_p(\boldsymbol{x}), \qquad \boldsymbol{x} \in \Gamma, \tag{3.3}$$

being $Z_\infty > 0$ real and constant throughout Γ, and $Z_p(\boldsymbol{x})$ a possibly complex-valued impedance that depends on the position $\boldsymbol{x}$ and that has a bounded support contained in Γ_p. The case of complex Z_∞ and k will be discussed later. If $Z = 0$ or $Z = \infty$, then we retrieve respectively the classical Neumann or Dirichlet boundary conditions. The scattered field u satisfies the non-homogeneous impedance boundary condition

$$-\frac{\partial u}{\partial n} + Z u = f_z \qquad \text{on } \Gamma, \tag{3.4}$$

where the impedance data function f_z is known, has its support contained in Γ_p, and is given, because of (3.2), by

$$f_z = \frac{\partial u_I}{\partial n} - Z u_I + \frac{\partial u_R}{\partial n} - Z u_R \qquad \text{on } \Gamma. \tag{3.5}$$

An outgoing radiation condition has to be also imposed for the scattered field u, which specifies its decaying behavior at infinity and eliminates the non-physical solutions, e.g., ingoing volume or surface waves. This radiation condition can be stated for $r \to \infty$ in a more adjusted way as

$$\begin{cases} |u| \le \dfrac{C}{\sqrt{r}} \quad \text{and} \quad \left|\dfrac{\partial u}{\partial r} - iku\right| \le \dfrac{C}{r} & \text{if } x_2 > \dfrac{1}{2Z_\infty}\ln(1+\beta r), \\ |u| \le C \quad \text{and} \quad \left|\dfrac{\partial u}{\partial r} - i\sqrt{Z_\infty^2 + k^2}\,u\right| \le \dfrac{C}{r} & \text{if } x_2 \le \dfrac{1}{2Z_\infty}\ln(1+\beta r), \end{cases} \tag{3.6}$$

for some constants $C > 0$, where $r = |\boldsymbol{x}|$ and $\beta = 8\pi k Z_\infty^2/(Z_\infty^2 + k^2)$. It implies that two different asymptotic behaviors can be established for the scattered field u, which are shown in Figure 3.2. Away from the boundary Γ and inside the domain Ω_e, the first expression in (3.6) dominates, which corresponds to a classical Sommerfeld radiation condition

like (C.8) and is associated with volume waves. Near the boundary, on the other hand, the second expression in (3.6) resembles a Sommerfeld radiation condition, but only along the boundary and having a different wave number, and is therefore related to the propagation of surface waves. It is often expressed also as

$$\left| \frac{\partial u}{\partial |x_1|} - i\sqrt{Z_\infty^2 + k^2}\, u \right| \leq \frac{C}{|x_1|}. \tag{3.7}$$

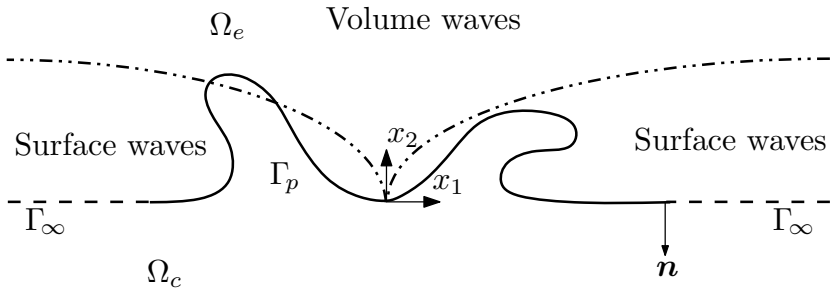

FIGURE 3.2. Asymptotic behaviors in the radiation condition.

Analogously as done by Durán, Muga & Nédélec (2005*a*, 2006), the radiation condition (3.6) can be stated alternatively as

$$\begin{cases} |u| \leq \dfrac{C}{\sqrt{r}} \quad \text{and} \quad \left| \dfrac{\partial u}{\partial r} - iku \right| \leq \dfrac{C}{r^{1-\alpha}} & \text{if } \; x_2 > Cr^\alpha, \\ |u| \leq C \quad \text{and} \quad \left| \dfrac{\partial u}{\partial r} - i\sqrt{Z_\infty^2 + k^2}\, u \right| \leq \dfrac{C}{r^{1-2\alpha}} & \text{if } \; x_2 \leq Cr^\alpha, \end{cases} \tag{3.8}$$

for $0 < \alpha < 1/2$ and some constants $C > 0$, being the growth of Cr^α bigger than the logarithmic one at infinity. Equivalently, the radiation condition can be expressed in a more weaker and general formulation as

$$\begin{cases} \lim\limits_{R\to\infty} \displaystyle\int_{S_R^1} |u|^2 \, \mathrm{d}\gamma < \infty \quad \text{and} \quad \lim\limits_{R\to\infty} \int_{S_R^1} \left| \frac{\partial u}{\partial r} - iku \right|^2 \mathrm{d}\gamma = 0, \\ \lim\limits_{R\to\infty} \displaystyle\int_{S_R^2} \frac{|u|^2}{\ln R} \, \mathrm{d}\gamma < \infty \quad \text{and} \quad \lim\limits_{R\to\infty} \int_{S_R^2} \frac{1}{\ln R} \left| \frac{\partial u}{\partial r} - i\sqrt{Z_\infty^2 + k^2}\, u \right|^2 \mathrm{d}\gamma = 0, \end{cases} \tag{3.9}$$

where

$$S_R^1 = \left\{ \boldsymbol{x} \in \mathbb{R}^2_+ : \, |\boldsymbol{x}| = R, \;\; x_2 > \frac{1}{2Z_\infty} \ln(1 + \beta R) \right\}, \tag{3.10}$$

$$S_R^2 = \left\{ \boldsymbol{x} \in \mathbb{R}^2_+ : \, |\boldsymbol{x}| = R, \;\; x_2 < \frac{1}{2Z_\infty} \ln(1 + \beta R) \right\}. \tag{3.11}$$

We observe that in this case

$$\int_{S_R^1} \mathrm{d}\gamma = \mathcal{O}(R) \qquad \text{and} \qquad \int_{S_R^2} \mathrm{d}\gamma = \mathcal{O}(\ln R). \tag{3.12}$$

The portions S_R^1 and S_R^2 of the half-circle and the terms depending on S_R^2 of the radiation condition (3.9) have to be modified when using instead the polynomial curves of (3.8). We refer to Stoker (1956) for a discussion on radiation conditions for surface waves.

The perturbed half-plane impedance Helmholtz problem can be finally stated as

$$\begin{cases} \text{Find } u : \Omega_e \to \mathbb{C} \text{ such that} \\ \Delta u + k^2 u = 0 \qquad \text{in } \Omega_e, \\ -\dfrac{\partial u}{\partial n} + Zu = f_z \qquad \text{on } \Gamma, \\ \text{+ Outgoing radiation condition as } |\boldsymbol{x}| \to \infty, \end{cases} \tag{3.13}$$

where the outgoing radiation condition is given by (3.6).

3.2.2 Incident and reflected field

To determine the incident field u_I and the reflected field u_R, we study the solutions u_T of the unperturbed and homogeneous wave propagation problem with neither a scattered field nor an associated radiation condition, being $u_T = u_I + u_R$. The solutions are searched in particular to be physically admissible, i.e., solutions which do not explode exponentially in the propagation domain, depicted in Figure 3.1. We analyze thus the half-plane impedance Helmholtz problem

$$\begin{cases} \Delta u_T + k^2 u_T = 0 \qquad \text{in } \mathbb{R}^2_+, \\ \dfrac{\partial u_T}{\partial x_2} + Z_\infty u_T = 0 \qquad \text{on } \{x_2 = 0\}. \end{cases} \tag{3.14}$$

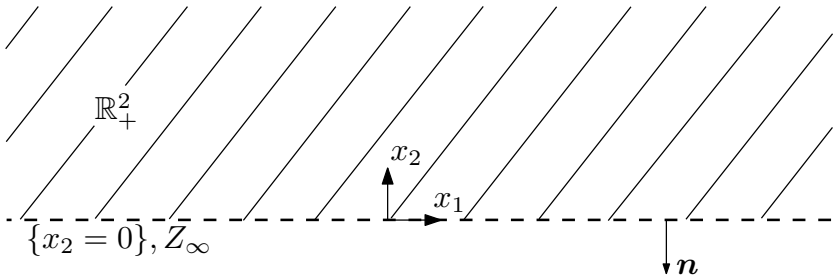

FIGURE 3.3. Positive half-plane $\mathbb{R}^2_+$.

Two different kinds of independent solutions u_T exist for the problem (3.14). They are obtained by studying the way how progressive plane waves of the form $e^{i\boldsymbol{k}\cdot\boldsymbol{x}}$ can be adjusted to satisfy the boundary condition, where the wave propagation vector $\boldsymbol{k} = (k_1, k_2)$ is such that $(\boldsymbol{k} \cdot \boldsymbol{k}) = k^2$.

The first kind of solution corresponds to a linear combination of two progressive plane volume waves and is given, up to an arbitrary multiplicative constant, by

$$u_T(\boldsymbol{x}) = e^{i\boldsymbol{k}\cdot\boldsymbol{x}} - \left(\frac{Z_\infty + ik_2}{Z_\infty - ik_2}\right) e^{i\bar{\boldsymbol{k}}\cdot\boldsymbol{x}}, \tag{3.15}$$

where $\boldsymbol{k} \in \mathbb{R}^2$ and $\bar{\boldsymbol{k}} = (k_1, -k_2)$. Due the involved physics, we consider that $k_2 \leq 0$. The first term of (3.15) can be interpreted as an incident plane volume wave, while the second term represents the reflected plane volume wave due the presence of the boundary with impedance. Thus

$$u_I(\boldsymbol{x}) = e^{i\boldsymbol{k}\cdot\boldsymbol{x}}, \tag{3.16}$$

$$u_R(\boldsymbol{x}) = -\left(\frac{Z_\infty + ik_2}{Z_\infty - ik_2}\right) e^{i\bar{\boldsymbol{k}}\cdot\boldsymbol{x}}. \tag{3.17}$$

It can be observed that the solution (3.15) vanishes when $k_2 = 0$, i.e., when the wave propagation is parallel to the half-plane's boundary. The wave propagation vector $\boldsymbol{k}$, by considering a parametrization through the angle of incidence θ_I for $0 \leq \theta_I \leq \pi$, can be expressed as $\boldsymbol{k} = (-k\cos\theta_I, -k\sin\theta_I)$. In this case the solution is described by

$$u_T(\boldsymbol{x}) = e^{-ik(x_1\cos\theta_I + x_2\sin\theta_I)} - \left(\frac{Z_\infty - ik\sin\theta_I}{Z_\infty + ik\sin\theta_I}\right) e^{-ik(x_1\cos\theta_I - x_2\sin\theta_I)}. \tag{3.18}$$

The second kind of solution, up to an arbitrary scaling factor, corresponds to a progressive plane surface wave, and is given by

$$u_T(\boldsymbol{x}) = u_I(\boldsymbol{x}) = e^{ik_s x_1} e^{-Z_\infty x_2}, \qquad k_s^2 = Z_\infty^2 + k^2. \tag{3.19}$$

It can be observed that plane surface waves correspond to plane volume waves with a complex wave propagation vector $\boldsymbol{k} = (k_s, iZ_\infty)$, are guided along the half-plane's boundary, and decrease exponentially towards its interior, hence their name. In this case there exists no reflected field, since the waves travel along the boundary. We remark that the plane surface waves vanish completely for classical Dirichlet ($Z_\infty = \infty$) or Neumann ($Z_\infty = 0$) boundary conditions.

3.3 Green's function

3.3.1 Problem definition

The Green's function represents the response of the unperturbed system to a Dirac mass. It corresponds to a function G, which depends on the wave number k, on the impedance Z_∞, on a fixed source point $\boldsymbol{x} \in \mathbb{R}^2_+$, and on an observation point $\boldsymbol{y} \in \mathbb{R}^2_+$. The Green's function is computed in the sense of distributions for the variable $\boldsymbol{y}$ in the half-plane $\mathbb{R}^2_+$ by placing at the right-hand side of the Helmholtz equation a Dirac mass $\delta_{\boldsymbol{x}}$, centered at the point $\boldsymbol{x}$. It is therefore a solution for the radiation problem of a point source,

namely

$$\left\{\begin{array}{ll} \text{Find } G(\boldsymbol{x},\cdot):\mathbb{R}^2_+\to\mathbb{C} \text{ such that} & \\ \Delta_{\boldsymbol{y}}G(\boldsymbol{x},\boldsymbol{y})+k^2G(\boldsymbol{x},\boldsymbol{y})=\delta_{\boldsymbol{x}}(\boldsymbol{y}) & \text{in } \mathcal{D}'(\mathbb{R}^2_+), \\ \dfrac{\partial G}{\partial y_2}(\boldsymbol{x},\boldsymbol{y})+Z_\infty G(\boldsymbol{x},\boldsymbol{y})=0 & \text{on } \{y_2=0\}, \\ \text{+ Outgoing radiation condition as } |\boldsymbol{y}|\to\infty. & \end{array}\right. \tag{3.20}$$

The outgoing radiation condition, in the same way as in (3.6), is given here as $|\boldsymbol{y}|\to\infty$ by

$$\left\{\begin{array}{ll} |G|\le\dfrac{C}{\sqrt{|\boldsymbol{y}|}} \quad \text{and} \quad \left|\dfrac{\partial G}{\partial r_{\boldsymbol{y}}}-ikG\right|\le\dfrac{C}{|\boldsymbol{y}|} & \text{if } y_2>\dfrac{\ln\big(1+\beta|\boldsymbol{y}|\big)}{2Z_\infty}, \\ |G|\le C \quad \text{and} \quad \left|\dfrac{\partial G}{\partial r_{\boldsymbol{y}}}-i\sqrt{Z_\infty^2+k^2}G\right|\le\dfrac{C}{|\boldsymbol{y}|} & \text{if } y_2\le\dfrac{\ln\big(1+\beta|\boldsymbol{y}|\big)}{2Z_\infty}, \end{array}\right. \tag{3.21}$$

for some constants $C>0$, independent of $r=|\boldsymbol{y}|$, where $\beta=8\pi kZ_\infty^2/(Z_\infty^2+k^2)$.

3.3.2 Special cases

When the Green's function problem (3.20) is solved using either homogeneous Dirichlet or Neumann boundary conditions, then its solution is found straightforwardly using the method of images (cf., e.g., Morse & Feshbach 1953).

a) Homogeneous Dirichlet boundary condition

We consider in the problem (3.20) the particular case of a homogeneous Dirichlet boundary condition, namely

$$G(\boldsymbol{x},\boldsymbol{y})=0, \qquad \boldsymbol{y}\in\{y_2=0\}, \tag{3.22}$$

which corresponds to the limit case when the impedance is infinite ($Z_\infty=\infty$). In this case, the Green's function G can be explicitly calculated using the method of images, since it has to be antisymmetric with respect to the axis $\{y_2=0\}$. An additional image source point $\bar{\boldsymbol{x}}=(x_1,-x_2)$, located on the lower half-plane and associated with a negative Dirac mass, is placed for this purpose just opposite to the upper half-plane's source point $\boldsymbol{x}=(x_1,x_2)$. The desired solution is then obtained by evaluating the full-plane Green's function (C.23) for each Dirac mass, which yields finally

$$G(\boldsymbol{x},\boldsymbol{y})=-\frac{i}{4}H_0^{(1)}\big(k|\boldsymbol{y}-\boldsymbol{x}|\big)+\frac{i}{4}H_0^{(1)}\big(k|\boldsymbol{y}-\bar{\boldsymbol{x}}|\big). \tag{3.23}$$

b) Homogeneous Neumann boundary condition

We consider in the problem (3.20) the particular case of a homogeneous Neumann boundary condition, namely

$$\frac{\partial G}{\partial n_{\boldsymbol{y}}}(\boldsymbol{x},\boldsymbol{y})=0, \qquad \boldsymbol{y}\in\{y_2=0\}, \tag{3.24}$$

which corresponds to the limit case when the impedance is zero ($Z_\infty=0$). As in the previous case, the method of images is again employed, but now the half-plane Green's function G has to be symmetric with respect to the axis $\{y_2=0\}$. Therefore, an additional

image source point $\bar{\boldsymbol{x}} = (x_1, -x_2)$, located on the lower half-plane, is placed just opposite to the upper half-plane's source point $\boldsymbol{x} = (x_1, x_2)$, but now associated with a positive Dirac mass. The desired solution is then obtained by evaluating the full-plane Green's function (C.23) for each Dirac mass, which yields

$$G(\boldsymbol{x}, \boldsymbol{y}) = -\frac{i}{4} H_0^{(1)}\big(k|\boldsymbol{y} - \boldsymbol{x}|\big) - \frac{i}{4} H_0^{(1)}\big(k|\boldsymbol{y} - \bar{\boldsymbol{x}}|\big). \tag{3.25}$$

3.3.3 Spectral Green's function

a) Boundary-value problem

To solve (3.20) in the general case, we use a modified partial Fourier transform on the horizontal y_1-axis, taking advantage of the fact that there is no horizontal variation in the geometry of the problem. To obtain the corresponding spectral Green's function, we follow the same procedure as the one performed in Durán et al. (2005*a*). We define the forward Fourier transform of a function $F\big(\boldsymbol{x}, (\cdot, y_2)\big) : \mathbb{R} \to \mathbb{C}$ by

$$\widehat{F}(\xi; y_2, x_2) = \frac{1}{\sqrt{2\pi}} \int_{-\infty}^{\infty} F(\boldsymbol{x}, \boldsymbol{y})\, e^{-i\xi(y_1 - x_1)}\, \mathrm{d}y_1, \qquad \xi \in \mathbb{R}, \tag{3.26}$$

and its inverse by

$$F(\boldsymbol{x}, \boldsymbol{y}) = \frac{1}{\sqrt{2\pi}} \int_{-\infty}^{\infty} \widehat{F}(\xi; y_2, x_2)\, e^{i\xi(y_1 - x_1)}\, \mathrm{d}\xi, \qquad y_1 \in \mathbb{R}. \tag{3.27}$$

To ensure a correct integration path for the Fourier transform and correct physical results, the calculations have to be performed in the framework of the limiting absorption principle, which allows to treat all the appearing integrals as Cauchy principal values. For this purpose, we take a small dissipation parameter $\varepsilon > 0$ into account and consider the problem (3.20) as the limit case when $\varepsilon \to 0$ of the dissipative problem

$$\begin{cases} \text{Find } G_\varepsilon(\boldsymbol{x}, \cdot) : \mathbb{R}^2_+ \to \mathbb{C} \text{ such that} \\ \Delta_{\boldsymbol{y}} G_\varepsilon(\boldsymbol{x}, \boldsymbol{y}) + k_\varepsilon^2 G_\varepsilon(\boldsymbol{x}, \boldsymbol{y}) = \delta_{\boldsymbol{x}}(\boldsymbol{y}) & \text{in } \mathcal{D}'(\mathbb{R}^2_+), \\ \dfrac{\partial G_\varepsilon}{\partial y_2}(\boldsymbol{x}, \boldsymbol{y}) + Z_\infty G_\varepsilon(\boldsymbol{x}, \boldsymbol{y}) = 0 & \text{on } \{y_2 = 0\}, \end{cases} \tag{3.28}$$

where $k_\varepsilon = k + i\varepsilon$. This choice ensures a correct outgoing dissipative volume-wave behavior. In the same way as for the Laplace equation, the impedance Z_∞ could be also incorporated into this dissipative framework, i.e., by considering $Z_\varepsilon = Z_\infty + i\varepsilon$, but it is not really necessary since the use of a dissipative wave number k_ε is enough to take care of all the appearing issues. Further references for the application of this principle can be found in Bonnet-BenDhia & Tillequin (2001), Hazard & Lenoir (1998), and Nosich (1994).

Applying thus the Fourier transform (3.26) on the system (3.28) leads to a linear second order ordinary differential equation for the variable y_2, with prescribed boundary values,

given by

$$\begin{cases} \dfrac{\partial^2 \widehat{G}_\varepsilon}{\partial y_2^2}(\xi) - (\xi^2 - k_\varepsilon^2)\widehat{G}_\varepsilon(\xi) = \dfrac{\delta(y_2 - x_2)}{\sqrt{2\pi}}, & y_2 > 0, \\ \dfrac{\partial \widehat{G}_\varepsilon}{\partial y_2}(\xi) + Z_\infty \widehat{G}_\varepsilon(\xi) = 0, & y_2 = 0. \end{cases} \tag{3.29}$$

We use the method of undetermined coefficients, and solve the homogeneous differential equation of the problem (3.29) respectively in the strip $\{\boldsymbol{y} \in \mathbb{R}^2_+ : 0 < y_2 < x_2\}$ and in the half-plane $\{\boldsymbol{y} \in \mathbb{R}^2_+ : y_2 > x_2\}$. This gives a solution for $\widehat{G}_\varepsilon$ in each domain, as a linear combination of two independent solutions of an ordinary differential equation, namely

$$\widehat{G}_\varepsilon(\xi) = \begin{cases} a\, e^{\sqrt{\xi^2 - k_\varepsilon^2}\, y_2} + b\, e^{-\sqrt{\xi^2 - k_\varepsilon^2}\, y_2} & \text{for } 0 < y_2 < x_2, \\ c\, e^{\sqrt{\xi^2 - k_\varepsilon^2}\, y_2} + d\, e^{-\sqrt{\xi^2 - k_\varepsilon^2}\, y_2} & \text{for } y_2 > x_2. \end{cases} \tag{3.30}$$

The unknowns a, b, c, and d, which depend on ξ and x_2, are determined through the boundary condition, by imposing continuity, and by assuming an outgoing wave behavior. The complex square root in (3.30) is defined in such a way that its real part is always positive.

b) Complex square roots

Due the application of the limiting absorption principle, the square root that appears in the general solution (3.30) has to be understood as a complex map $\xi \mapsto \sqrt{\xi^2 - k_\varepsilon^2}$, which is decomposed as the product between $\sqrt{\xi - k_\varepsilon}$ and $\sqrt{\xi + k_\varepsilon}$, and has its two analytic branch cuts on the complex ξ plane defined in such a way that they do not intersect the real axis. Further details on complex branch cuts can be found in the books of Bak & Newman (1997) and Felsen & Marcuwitz (2003). The arguments are taken in such a way that $\arg(\xi - k_\varepsilon) \in (-\frac{3\pi}{2}, \frac{\pi}{2})$ for the map $\sqrt{\xi - k_\varepsilon}$, and $\arg(\xi + k_\varepsilon) \in (-\frac{\pi}{2}, \frac{3\pi}{2})$ for the map $\sqrt{\xi + k_\varepsilon}$. These maps can be therefore defined by (Durán et al. 2005*a*)

$$\sqrt{\xi - k_\varepsilon} = -i\sqrt{|k_\varepsilon|}\, e^{\frac{i}{2}\arg(k_\varepsilon)} \exp\left(\frac{1}{2}\int_0^\xi \frac{\mathrm{d}\eta}{\eta - k_\varepsilon}\right), \tag{3.31}$$

and

$$\sqrt{\xi + k_\varepsilon} = \sqrt{|k_\varepsilon|}\, e^{\frac{i}{2}\arg(k_\varepsilon)} \exp\left(\frac{1}{2}\int_0^\xi \frac{\mathrm{d}\eta}{\eta + k_\varepsilon}\right). \tag{3.32}$$

Consequently $\sqrt{\xi^2 - k_\varepsilon^2}$ is even and analytic in the domain shown in Figure 3.4. It can be hence defined by

$$\sqrt{\xi^2 - k_\varepsilon^2} = \sqrt{\xi - k_\varepsilon}\,\sqrt{\xi + k_\varepsilon} = -ik_\varepsilon \exp\left(\int_0^\xi \frac{\eta}{\eta^2 - k_\varepsilon^2}\,\mathrm{d}\eta\right), \tag{3.33}$$

and is characterized, for $\xi, k \in \mathbb{R}$, by

$$\sqrt{\xi^2 - k^2} = \begin{cases} \sqrt{\xi^2 - k^2}, & \xi^2 \geq k^2, \\ -i\sqrt{k^2 - \xi^2}, & \xi^2 < k^2. \end{cases} \tag{3.34}$$

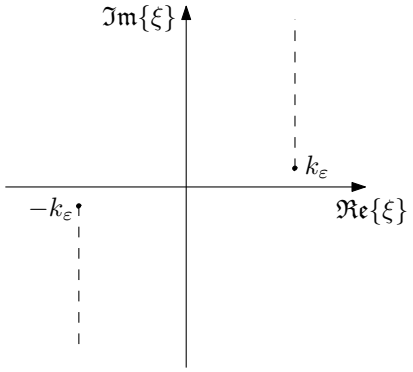

FIGURE 3.4. Analytic branch cuts of the complex map $\sqrt{\xi^2 - k_\varepsilon^2}$.

We remark that if $\xi \in \mathbb{R}$, then $\arg(\xi - k_\varepsilon) \in (-\pi, 0)$ and $\arg(\xi + k_\varepsilon) \in (0, \pi)$. This proceeds from the fact that $\arg(k_\varepsilon) \in (0, \pi)$, since by the limiting absorption principle it holds that $\mathfrak{Im}\{k_\varepsilon\} = \varepsilon > 0$. Thus $\arg\left(\sqrt{\xi - k_\varepsilon}\right) \in (-\frac{\pi}{2}, 0)$, $\arg\left(\sqrt{\xi + k_\varepsilon}\right) \in (0, \frac{\pi}{2})$, and $\arg\left(\sqrt{\xi^2 - k_\varepsilon^2}\right) \in (-\frac{\pi}{2}, \frac{\pi}{2})$. Hence, the real part of the complex map $\sqrt{\xi^2 - k_\varepsilon^2}$ for real ξ is strictly positive, i.e., $\mathfrak{Re}\left\{\sqrt{\xi^2 - k_\varepsilon^2}\right\} > 0$. Therefore the function $e^{-\sqrt{\xi^2 - k_\varepsilon^2}\, y_2}$ is even and exponentially decreasing as $y_2 \to \infty$.

c) Spectral Green's function with dissipation

Now, thanks to (3.30), the computation of $\widehat{G}_\varepsilon$ is straightforward. From the boundary condition of (3.29) a relation for the coefficients a and b can be derived, which is given by

$$a\left(Z_\infty + \sqrt{\xi^2 - k_\varepsilon^2}\right) + b\left(Z_\infty - \sqrt{\xi^2 - k_\varepsilon^2}\right) = 0. \tag{3.35}$$

On the other hand, since the solution (3.30) has to be bounded at infinity as $y_2 \to \infty$, and since $\mathfrak{Re}\left\{\sqrt{\xi^2 - k_\varepsilon^2}\right\} > 0$, it follows then necessarily that

$$c = 0. \tag{3.36}$$

To ensure the continuity of the Green's function at the point $y_2 = x_2$, it is needed that

$$d = a\, e^{\sqrt{\xi^2 - k_\varepsilon^2}\, 2x_2} + b. \tag{3.37}$$

Using relations (3.35), (3.36), and (3.37) in (3.30), we obtain the expression

$$\widehat{G}_\varepsilon(\xi) = a\, e^{\sqrt{\xi^2 - k_\varepsilon^2}\, x_2}\left[e^{-\sqrt{\xi^2 - k_\varepsilon^2}\,|y_2 - x_2|} - \left(\frac{Z_\infty + \sqrt{\xi^2 - k_\varepsilon^2}}{Z_\infty - \sqrt{\xi^2 - k_\varepsilon^2}}\right) e^{-\sqrt{\xi^2 - k_\varepsilon^2}\,(y_2 + x_2)}\right]. \tag{3.38}$$

The remaining unknown coefficient a is determined by replacing (3.38) in the differential equation of (3.29), taking the derivatives in the sense of distributions, particularly

$$\frac{\partial}{\partial y_2}\left\{e^{-\sqrt{\xi^2 - k_\varepsilon^2}\,|y_2 - x_2|}\right\} = -\sqrt{\xi^2 - k_\varepsilon^2}\, \operatorname{sign}(y_2 - x_2)\, e^{-\sqrt{\xi^2 - k_\varepsilon^2}\,|y_2 - x_2|}, \tag{3.39}$$

and

$$\frac{\partial}{\partial y_2}\big\{\operatorname{sign}(y_2 - x_2)\big\} = 2\,\delta(y_2 - x_2). \tag{3.40}$$

So, the second derivative of (3.38) becomes

$$\frac{\partial^2 \widehat{G}_\varepsilon}{\partial y_2^2}(\xi) = a\, e^{\sqrt{\xi^2-k_\varepsilon^2}\, x_2} \Bigg[(\xi^2 - k_\varepsilon^2)\, e^{-\sqrt{\xi^2-k_\varepsilon^2}\,|y_2-x_2|} - 2\sqrt{\xi^2-k_\varepsilon^2}\,\delta(y_2-x_2) \\ - \left(\frac{Z_\infty + \sqrt{\xi^2-k_\varepsilon^2}}{Z_\infty - \sqrt{\xi^2-k_\varepsilon^2}} \right) (\xi^2 - k_\varepsilon^2)\, e^{-\sqrt{\xi^2-k_\varepsilon^2}\,(y_2+x_2)} \Bigg]. \tag{3.41}$$

This way, from (3.38) and (3.41) in the first equation of (3.29), we obtain that

$$a = -\frac{e^{-\sqrt{\xi^2-k_\varepsilon^2}\, x_2}}{\sqrt{8\pi}\,\sqrt{\xi^2-k_\varepsilon^2}}. \tag{3.42}$$

Finally, the spectral Green's function $\widehat{G}_\varepsilon$ with dissipation ε is given by

$$\widehat{G}_\varepsilon(\xi; y_2, x_2) = -\frac{e^{-\sqrt{\xi^2-k_\varepsilon^2}\,|y_2-x_2|}}{\sqrt{8\pi}\sqrt{\xi^2-k_\varepsilon^2}} + \left(\frac{Z_\infty + \sqrt{\xi^2-k_\varepsilon^2}}{Z_\infty - \sqrt{\xi^2-k_\varepsilon^2}} \right) \frac{e^{-\sqrt{\xi^2-k_\varepsilon^2}\,(y_2+x_2)}}{\sqrt{8\pi}\sqrt{\xi^2-k_\varepsilon^2}}. \tag{3.43}$$

d) Analysis of singularities

To obtain the spectral Green's function $\widehat{G}$ without dissipation, the limit $\varepsilon \to 0$ has to be taken in (3.43). This can be done directly wherever the limit is regular and continuous on ξ. Singular points, on the other hand, have to be analyzed carefully to fulfill correctly the limiting absorption principle. Thus we study first the singularities of the limit function before applying this principle, i.e., considering just $\varepsilon = 0$, in which case we have

$$\widehat{G}_0(\xi) = -\frac{e^{-\sqrt{\xi^2-k^2}\,|y_2-x_2|}}{\sqrt{8\pi}\sqrt{\xi^2-k^2}} + \left(\frac{Z_\infty + \sqrt{\xi^2-k^2}}{Z_\infty - \sqrt{\xi^2-k^2}} \right) \frac{e^{-\sqrt{\xi^2-k^2}\,(y_2+x_2)}}{\sqrt{8\pi}\sqrt{\xi^2-k^2}}. \tag{3.44}$$

Possible singularities for (3.44) may only appear when $|\xi| = k$ or when $|\xi| = \xi_p$, being $\xi_p = \sqrt{Z_\infty^2 + k^2}$, i.e., when the denominator of the fractions is zero. Otherwise the function is regular and continuous.

For $\xi = k$ and $\xi = -k$ the function (3.44) is continuous. This can be seen by writing it, analogously as in Durán, Muga & Nédélec (2006), in the form

$$\widehat{G}_0(\xi) = \frac{H\big(g(\xi)\big)}{g(\xi)}, \tag{3.45}$$

where

$$g(\xi) = \sqrt{\xi^2 - k^2}, \tag{3.46}$$

and

$$H(\beta) = \frac{1}{\sqrt{8\pi}} \left(-e^{-\beta\,|y_2-x_2|} + \frac{Z_\infty + \beta}{Z_\infty - \beta}\, e^{-\beta\,(y_2+x_2)} \right), \qquad \beta \in \mathbb{C}. \tag{3.47}$$

Since $H(\beta)$ is an analytic function in $\beta = 0$, since $H(0) = 0$, and since

$$\lim_{\xi \to \pm k} \widehat{G}_0(\xi) = \lim_{\xi \to \pm k} \frac{H\big(g(\xi)\big) - H(0)}{g(\xi)} = H'(0), \tag{3.48}$$

we can easily obtain that

$$\lim_{\xi\to\pm k}\widehat{G}_0(\xi)=\frac{1}{\sqrt{8\pi}}\left(1+\frac{1}{Z_\infty}+|y_2-x_2|-(y_2+x_2)\right), \tag{3.49}$$

being thus $\widehat{G}_0$ bounded and continuous on $\xi=k$ and $\xi=-k$.

For $\xi=\xi_p$ and $\xi=-\xi_p$, where $\xi_p=\sqrt{Z_\infty^2+k^2}$, the function (3.44) presents two simple poles, whose residues are characterized by

$$\lim_{\xi\to\pm\xi_p}(\xi\mp\xi_p)\,\widehat{G}_0(\xi)=\mp\frac{Z_\infty}{\sqrt{2\pi}\,\xi_p}\,e^{-Z_\infty(y_2+x_2)}. \tag{3.50}$$

To analyze the effect of these singularities, we have to study the computation of the inverse Fourier transform of

$$\widehat{G}_P(\xi)=\frac{Z_\infty}{\sqrt{2\pi}\,\xi_p}\,e^{-Z_\infty(y_2+x_2)}\left(\frac{1}{\xi+\xi_p}-\frac{1}{\xi-\xi_p}\right), \tag{3.51}$$

which has to be done in the frame of the limiting absorption principle to obtain the correct physical results, i.e., the inverse Fourier transform has to be understood in the sense of

$$G_P(\boldsymbol{x},\boldsymbol{y})=\lim_{\varepsilon\to0}\left\{\frac{Z_\infty}{2\pi\xi_p}\,e^{-Z_\infty(y_2+x_2)}\int_{-\infty}^{\infty}\left(\frac{1}{\xi+\xi_p}-\frac{1}{\xi-\xi_p}\right)e^{i\xi(y_1-x_1)}\mathrm{d}\xi\right\}, \tag{3.52}$$

where now $\xi_p=\sqrt{Z_\infty^2+k_\varepsilon^2}$, which is such that $\mathfrak{Im}\{\xi_p\}>0$.

To perform correctly the computation of (3.52), we apply the residue theorem of complex analysis (cf., e.g., Arfken & Weber 2005, Bak & Newman 1997, Dettman 1984) on the complex meromorphic mapping

$$F(\xi)=\left(\frac{1}{\xi+\xi_p}-\frac{1}{\xi-\xi_p}\right)e^{i\xi(y_1-x_1)}, \tag{3.53}$$

which admits two simple poles at ξ_p and $-\xi_p$, where $\mathfrak{Im}\{\xi_p\}>0$. We already did this computation for the Laplace equation and obtained the expression (2.59), namely

$$\int_{-\infty}^{\infty}F(\xi)\,\mathrm{d}\xi=-i2\pi e^{i\xi_p|y_1-x_1|},\qquad(y_1-x_1)\in\mathbb{R}. \tag{3.54}$$

Using (3.54) for $\xi_p=\sqrt{Z_\infty^2+k^2}$ yields that the inverse Fourier transform of (3.51), when considering the limiting absorption principle, is given by

$$G_P^L(\boldsymbol{x},\boldsymbol{y})=-\frac{iZ_\infty}{\xi_p}\,e^{-Z_\infty(y_2+x_2)}e^{i\xi_p|y_1-x_1|}. \tag{3.55}$$

We observe that this expression describes the asymptotic behavior of the surface waves, which are linked to the presence of the poles in the spectral Green's function.

If the limiting absorption principle is not considered, i.e., if $\mathfrak{Im}\{\xi_p\}=0$, then the inverse Fourier transform of (3.51) could be again computed in the sense of the principal value with the residue theorem. In this case we would obtain, instead of (3.54) and just as the expression (2.61) for the Laplace equation, the quantity

$$\int_{-\infty}^{\infty}F(\xi)\,\mathrm{d}\xi=2\pi\sin\big(\xi_p|y_1-x_1|\big),\qquad(y_1-x_1)\in\mathbb{R}. \tag{3.56}$$

The inverse Fourier transform of (3.51) would be in this case

$$G_P^{NL}(\boldsymbol{x},\boldsymbol{y}) = \frac{Z_\infty}{\xi_p}\, e^{-Z_\infty(y_2+x_2)} \sin\big(\xi_p|y_1-x_1|\big), \tag{3.57}$$

which is correct from the mathematical point of view, but yields only a standing surface wave, and not a desired outgoing progressive surface wave as in (3.55).

The effect of the limiting absorption principle, in the spatial dimension, is then given by the difference between (3.55) and (3.57), i.e., by

$$G_L(\boldsymbol{x},\boldsymbol{y}) = G_P^{L}(\boldsymbol{x},\boldsymbol{y}) - G_P^{NL}(\boldsymbol{x},\boldsymbol{y}) = -\frac{iZ_\infty}{\xi_p}\, e^{-Z_\infty(y_2+x_2)} \cos\big(\xi_p(y_1-x_1)\big), \tag{3.58}$$

whose Fourier transform, and therefore the spectral effect, is given by

$$\widehat{G}_L(\xi) = \widehat{G}_P^{L}(\xi) - \widehat{G}_P^{NL}(\xi) = -\frac{iZ_\infty}{\xi_p}\sqrt{\frac{\pi}{2}}\, e^{-Z_\infty(y_2+x_2)} \big[\delta(\xi-\xi_p)+\delta(\xi+\xi_p)\big]. \tag{3.59}$$

e) Spectral Green's function without dissipation

The spectral Green's function $\widehat{G}$ without dissipation is therefore obtained by taking the limit $\varepsilon \to 0$ in (3.43) and considering the effect of the limiting absorption principle for the appearing singularities, summarized in (3.59). Thus we obtain in the sense of distributions

$$\begin{aligned}\widehat{G}(\xi;y_2,x_2) = &-\frac{e^{-\sqrt{\xi^2-k^2}\,|y_2-x_2|}}{\sqrt{8\pi}\sqrt{\xi^2-k^2}} + \left(\frac{Z_\infty+\sqrt{\xi^2-k^2}}{Z_\infty-\sqrt{\xi^2-k^2}}\right)\frac{e^{-\sqrt{\xi^2-k^2}\,(y_2+x_2)}}{\sqrt{8\pi}\sqrt{\xi^2-k^2}} \\ &- \frac{iZ_\infty}{\xi_p}\sqrt{\frac{\pi}{2}}\, e^{-Z_\infty(y_2+x_2)} \big[\delta(\xi-\xi_p)+\delta(\xi+\xi_p)\big].\end{aligned} \tag{3.60}$$

For our further analysis, this spectral Green's function is decomposed into four terms according to

$$\widehat{G} = \widehat{G}_\infty + \widehat{G}_D + \widehat{G}_L + \widehat{G}_R, \tag{3.61}$$

where

$$\widehat{G}_\infty(\xi;y_2,x_2) = -\frac{e^{-\sqrt{\xi^2-k^2}\,|y_2-x_2|}}{\sqrt{8\pi}\sqrt{\xi^2-k^2}}, \tag{3.62}$$

$$\widehat{G}_D(\xi;y_2,x_2) = \frac{e^{-\sqrt{\xi^2-k^2}\,(y_2+x_2)}}{\sqrt{8\pi}\sqrt{\xi^2-k^2}}, \tag{3.63}$$

$$\widehat{G}_L(\xi;y_2,x_2) = -\frac{iZ_\infty}{\xi_p}\sqrt{\frac{\pi}{2}}\, e^{-Z_\infty(y_2+x_2)} \big[\delta(\xi-\xi_p)+\delta(\xi+\xi_p)\big], \tag{3.64}$$

$$\widehat{G}_R(\xi;y_2,x_2) = \frac{e^{-\sqrt{\xi^2-k^2}\,(y_2+x_2)}}{\sqrt{2\pi}\left(Z_\infty-\sqrt{\xi^2-k^2}\right)}. \tag{3.65}$$

3.3.4 Spatial Green's function

a) Spatial Green's function as an inverse Fourier transform

The desired spatial Green's function is then given by the inverse Fourier transform of the spectral Green's function (3.60), namely by

$$\begin{aligned} G(\boldsymbol{x},\boldsymbol{y}) = &-\frac{1}{4\pi}\int_{-\infty}^{\infty}\frac{e^{-\sqrt{\xi^2-k^2}\,|y_2-x_2|}}{\sqrt{\xi^2-k^2}}\,e^{i\xi(y_1-x_1)}\mathrm{d}\xi \\ &+\frac{1}{4\pi}\int_{-\infty}^{\infty}\left(\frac{Z_\infty+\sqrt{\xi^2-k^2}}{Z_\infty-\sqrt{\xi^2-k^2}}\right)\frac{e^{-\sqrt{\xi^2-k^2}\,(y_2+x_2)}}{\sqrt{\xi^2-k^2}}\,e^{i\xi(y_1-x_1)}\mathrm{d}\xi \\ &-\frac{iZ_\infty}{\xi_p}\,e^{-Z_\infty(y_2+x_2)}\cos\big(\xi_p(y_1-x_1)\big). \end{aligned} \tag{3.66}$$

Due the linearity of the Fourier transform, the decomposition (3.61) applies also in the spatial domain, i.e., the spatial Green's function is decomposed in the same manner by

$$G = G_\infty + G_D + G_L + G_R. \tag{3.67}$$

b) Term of the full-plane Green's function

The first term in (3.66) corresponds to the inverse Fourier transform of (3.62), and is given by

$$G_\infty(\boldsymbol{x},\boldsymbol{y}) = -\frac{1}{4\pi}\int_{-\infty}^{\infty}\frac{e^{-\sqrt{\xi^2-k^2}\,|y_2-x_2|}}{\sqrt{\xi^2-k^2}}\,e^{i\xi(y_1-x_1)}\mathrm{d}\xi. \tag{3.68}$$

The value for this integral can be derived either from Magnus & Oberhettinger (1954, page 33 or 118), from Gradshteyn & Ryzhik (2007, equations 3.914–4 or 6.616–3), or from Bateman (1954, equation 1.13–59), and yields the result that

$$-\frac{1}{4\pi}\int_{-\infty}^{\infty}\frac{e^{-\sqrt{\xi^2-k^2}\,|y_2-x_2|}}{\sqrt{\xi^2-k^2}}\,e^{i\xi(y_1-x_1)}\,\mathrm{d}\xi = -\frac{i}{4}H_0^{(1)}\big(k|\boldsymbol{y}-\boldsymbol{x}|\big), \tag{3.69}$$

being $H_0^{(1)}$ the zeroth order Hankel function of the first kind (vid. Subsection A.2.4). This way, the inverse Fourier transform of (3.62) is readily given by

$$G_\infty(\boldsymbol{x},\boldsymbol{y}) = -\frac{i}{4}H_0^{(1)}\big(k|\boldsymbol{y}-\boldsymbol{x}|\big). \tag{3.70}$$

We observe that (3.70) is, in fact, the full-plane Green's function of the Helmholtz equation. Thus $G_D + G_L + G_R$ represents the perturbation of the full-plane Green's function G_∞ due the presence of the impedance half-plane.

c) Term associated with a Dirichlet boundary condition

The inverse Fourier transform of (3.63) is computed in the same manner as the term G_∞. It is given by

$$G_D(\boldsymbol{x},\boldsymbol{y}) = \frac{1}{4\pi}\int_{-\infty}^{\infty}\frac{e^{-\sqrt{\xi^2-k^2}\,(y_2+x_2)}}{\sqrt{\xi^2-k^2}}\,e^{i\xi(y_1-x_1)}\mathrm{d}\xi, \tag{3.71}$$

and in this case, instead of (3.69), we consider the relation

$$\frac{1}{4\pi}\int_{-\infty}^{\infty}\frac{e^{-\sqrt{\xi^2-k^2}\,(y_2+x_2)}}{\sqrt{\xi^2-k^2}}\,e^{i\xi(y_1-x_1)}\,\mathrm{d}\xi=\frac{i}{4}H_0^{(1)}\big(k|\boldsymbol{y}-\bar{\boldsymbol{x}}|\big),\tag{3.72}$$

where $\bar{\boldsymbol{x}}=(x_1,-x_2)$ corresponds to the image point of $\boldsymbol{x}$ in the lower half-plane. The inverse Fourier transform of (3.63) is therefore given by

$$G_D(\boldsymbol{x},\boldsymbol{y})=\frac{i}{4}H_0^{(1)}\big(k|\boldsymbol{y}-\bar{\boldsymbol{x}}|\big),\tag{3.73}$$

which represents the additional term that appears in the Green's function due the method of images when considering a Dirichlet boundary condition, as in (3.23).

d) Term associated with the limiting absorption principle

The term G_L, the inverse Fourier transform of (3.64), is associated with the effect of the limiting absorption principle on the Green's function, and has been already calculated in (3.58). It is given by

$$G_L(\boldsymbol{x},\boldsymbol{y})=-\frac{iZ_\infty}{\xi_p}\,e^{-Z_\infty(y_2+x_2)}\cos\big(\xi_p(y_1-x_1)\big).\tag{3.74}$$

e) Remaining term

The remaining term G_R, the inverse Fourier transform of (3.65), can be computed as the integral

$$G_R(\boldsymbol{x},\boldsymbol{y})=\frac{1}{2\pi}\int_{-\infty}^{\infty}\frac{e^{-\sqrt{\xi^2-k^2}\,(y_2+x_2)}}{Z_\infty-\sqrt{\xi^2-k^2}}\,e^{i\xi(y_1-x_1)}\,\mathrm{d}\xi.\tag{3.75}$$

To simplify the notation, we define

$$v_1=y_1-x_1\qquad\text{and}\qquad v_2=y_2+x_2,\tag{3.76}$$

and we consider

$$G_R(\boldsymbol{x},\boldsymbol{y})=e^{-Z_\infty v_2}G_B(v_1,v_2),\tag{3.77}$$

where

$$G_B(v_1,v_2)=\frac{e^{Z_\infty v_2}}{2\pi}\int_{-\infty}^{\infty}\frac{e^{-\sqrt{\xi^2-k^2}\,v_2}}{Z_\infty-\sqrt{\xi^2-k^2}}\,e^{i\xi v_1}\,\mathrm{d}\xi.\tag{3.78}$$

From the derivative of (3.72) with respect to y_2 we obtain that

$$\frac{1}{4\pi}\int_{-\infty}^{\infty}e^{-\sqrt{\xi^2-k^2}\,v_2}e^{i\xi v_1}\,\mathrm{d}\xi=\frac{ik}{4}H_1^{(1)}\big(k|\boldsymbol{y}-\bar{\boldsymbol{x}}|\big)\frac{v_2}{|\boldsymbol{y}-\bar{\boldsymbol{x}}|}.\tag{3.79}$$

Due (3.79), we have for the y_2-derivative of G_B that

$$\frac{\partial G_B}{\partial y_2}(v_1,v_2)=\frac{e^{Z_\infty v_2}}{2\pi}\int_{-\infty}^{\infty}e^{-\sqrt{\xi^2-k^2}\,v_2}e^{i\xi v_1}\,\mathrm{d}\xi=\frac{ik}{2}H_1^{(1)}\big(k|\boldsymbol{y}-\bar{\boldsymbol{x}}|\big)\frac{v_2\,e^{Z_\infty v_2}}{|\boldsymbol{y}-\bar{\boldsymbol{x}}|}.\tag{3.80}$$

The value of the inverse Fourier transform (3.75) can be thus obtained by means of the primitive with respect to y_2 of (3.80), i.e.,

$$G_R(\boldsymbol{x},\boldsymbol{y})=\frac{ik}{2}\,e^{-Z_\infty v_2}\int_{-\infty}^{v_2}H_1^{(1)}\Big(k\sqrt{v_1^2+\eta^2}\Big)\,\frac{\eta\,e^{Z_\infty\eta}}{\sqrt{v_1^2+\eta^2}}\,\mathrm{d}\eta.\tag{3.81}$$

The expression (3.81) contains an integral with an unbounded lower limit, but even so, due the exponential decrease of its integrand, it could be adapted to be well suited for numerical evaluation, as is done, e.g., in Chapter V. Its advantage lies in the fact that it expresses intuitively the term G_R as a primitive of known functions. We observe that further related expressions can be obtained through integration by parts, e.g.,

$$G_R(\boldsymbol{x},\boldsymbol{y}) = -\frac{i}{2}H_0^{(1)}\big(k|\boldsymbol{y}-\bar{\boldsymbol{x}}|\big) + \frac{iZ_\infty}{2}\,e^{-Z_\infty v_2}\int_{-\infty}^{v_2} H_0^{(1)}\Big(k\sqrt{v_1^2+\eta^2}\Big)\,e^{Z_\infty \eta}\,\mathrm{d}\eta. \quad (3.82)$$

Formulae of this kind seem to be absent in the literature, but they resemble in their structure the expressions described in Ochmann (2004) and Ochmann & Brick (2008) for the three-dimensional case.

In Hein (2006, 2007) and Durán, Hein & Nédélec (2007*b*), the remaining term G_R was computed numerically by using an inverse fast Fourier transform (IFFT) for the expression (3.75). In our case, due parity, we can consider the equivalent expression

$$G_R(\boldsymbol{x},\boldsymbol{y}) = \frac{1}{\pi}\int_0^\infty \frac{e^{-\sqrt{\xi^2-k^2}\,v_2}}{Z_\infty-\sqrt{\xi^2-k^2}}\cos(\xi v_1)\,\mathrm{d}\xi, \quad (3.83)$$

which can be likewise treated by using numerical integration. In both cases, the involved integrals become divergent when $v_2 < 0$. We note that the expression (3.83) has the advantage of requiring only half as many values as the one considered for the IFFT. It can be also observed that (3.75) and (3.83) are slowly decreasing when $v_2 = 0$ and decrease exponentially when $v_2 > 0$.

To obtain an expression that is practical for numerical computation and which holds for all $v_2 \in \mathbb{R}$, similarly as in Pidcock (1985), we can separate (3.81) according to

$$G_R(\boldsymbol{x},\boldsymbol{y}) = e^{-Z_\infty v_2}\left(G_B(v_1,0) + \frac{ik}{2}\int_0^{v_2} H_1^{(1)}\Big(k\sqrt{v_1^2+\eta^2}\Big)\,\frac{\eta\,e^{Z_\infty\eta}}{\sqrt{v_1^2+\eta^2}}\,\mathrm{d}\eta\right), \quad (3.84)$$

where

$$G_B(v_1,0) = \frac{1}{\pi}\int_0^\infty \frac{\cos(\xi v_1)}{Z_\infty-\sqrt{\xi^2-k^2}}\,\mathrm{d}\xi. \quad (3.85)$$

The expression (3.84) is valid for any $v_2 \in \mathbb{R}$ and it can be computed numerically without difficulty since the integration limits are bounded.

It remains to be discussed how to compute effectively (3.83) and (3.85), which requires to isolate the poles of the spectral Green's function and to treat adequately the slow decrease at infinity when $v_2 = 0$. When the impedance is comparatively bigger than the wave number, i.e., when $|Z_\infty| > |k|$, then both goals can be obtained simultaneously by considering the fact that

$$\frac{Z_\infty}{\pi\xi_p}\int_0^\infty \frac{e^{-Z_\infty\xi v_2/\xi_p}}{\xi_p-\xi}\cos(\xi v_1)\,\mathrm{d}\xi = \frac{Z_\infty}{2\pi\xi_p}\,e^{-Z_\infty v_2}\Big\{e^{i\xi_p v_1}\,\mathrm{Ei}(Z_\infty v_2 - i\xi_p v_1) + e^{-i\xi_p v_1}\,\mathrm{Ei}(Z_\infty v_2 + i\xi_p v_1)\Big\}. \quad (3.86)$$

which is computed analogously as done for the Laplace equation in (2.93). The expression in the left-hand side of (3.86) contains completely the behavior of the poles in the spectral domain and includes most of the slow decrease at infinity, which improves as $|Z_\infty| \to \infty$. As a consequence, (3.83) can be computed more effectively as

$$G_R(\boldsymbol{x},\boldsymbol{y}) = \frac{1}{\pi}\int_0^\infty \left(\frac{e^{-\sqrt{\xi^2-k^2}\,v_2}}{Z_\infty - \sqrt{\xi^2-k^2}} - \frac{Z_\infty}{\xi_p}\,\frac{e^{-Z_\infty \xi v_2/\xi_p}}{\xi_p - \xi} \right) \cos(\xi v_1)\,\mathrm{d}\xi$$
$$+ \frac{Z_\infty}{2\pi\xi_p}\,e^{-Z_\infty v_2}\Big\{ e^{i\xi_p v_1}\,\mathrm{Ei}(Z_\infty v_2 - i\xi_p v_1) + e^{-i\xi_p v_1}\,\mathrm{Ei}(Z_\infty v_2 + i\xi_p v_1)\Big\}, \quad (3.87)$$

where Ei denotes the exponential integral function (vid. Subsection A.2.3). The integral in (3.87) is computed numerically. When the impedance is smaller than the wave number, i.e., when $|Z_\infty| < |k|$, then the expression inside the integral in (3.87) does no longer behave so well numerically and it becomes more convenient to remove the poles and the slow decrease independently. For the poles, as computed in (2.59), it holds that

$$\frac{2Z_\infty}{\pi}\,e^{-Z_\infty v_2}\int_0^\infty \frac{\cos(\xi v_1)}{\xi_p^2 - \xi^2}\,\mathrm{d}\xi = -\frac{iZ_\infty}{\xi_p}\,e^{-Z_\infty v_2}e^{i\xi_p|v_1|}. \quad (3.88)$$

When k is near the real axis, then for the slow decrease at infinity it holds that

$$\frac{1}{\pi}\int_0^\infty \frac{e^{-\sqrt{\xi^2+k^2}\,v_2}}{\sqrt{\xi^2+k^2}}\cos(\xi v_1)\,\mathrm{d}\xi = \frac{i}{2}H_0^{(1)}\big(ik|\boldsymbol{y}-\bar{\boldsymbol{x}}|\big) = \frac{1}{\pi}K_0\big(k|\boldsymbol{y}-\bar{\boldsymbol{x}}|\big), \quad (3.89)$$

where K_0 denotes the modified Bessel function of the second kind of order zero (vid. Subsection A.2.5). Hence, when $|Z_\infty| < |k|$ and $\arg(k) < \pi/4$, then (3.83) can be computed more effectively as

$$G_R(\boldsymbol{x},\boldsymbol{y}) = \frac{1}{\pi}\int_0^\infty \left(\frac{e^{-\sqrt{\xi^2-k^2}\,v_2}}{Z_\infty - \sqrt{\xi^2-k^2}} - \frac{2Z_\infty e^{-Z_\infty v_2}}{\xi_p^2-\xi^2} - \frac{e^{-\sqrt{\xi^2+k^2}\,v_2}}{\sqrt{\xi^2+k^2}} \right)\cos(\xi v_1)\,\mathrm{d}\xi$$
$$- \frac{iZ_\infty}{\xi_p}\,e^{-Z_\infty v_2}e^{i\xi_p|v_1|} + \frac{i}{2}H_0^{(1)}\big(ik|\boldsymbol{y}-\bar{\boldsymbol{x}}|\big). \quad (3.90)$$

When k is near the imaginary axis, then instead of (3.89) it is better to consider for the slow decrease at infinity the expression

$$\frac{1}{\pi}\int_0^\infty \frac{e^{-\sqrt{\xi^2-k^2}\,v_2}}{\sqrt{\xi^2-k^2}}\cos(\xi v_1)\,\mathrm{d}\xi = \frac{i}{2}H_0^{(1)}\big(k|\boldsymbol{y}-\bar{\boldsymbol{x}}|\big), \quad (3.91)$$

Now, when $|Z_\infty| < |k|$ and $\arg(k) > \pi/4$, then (3.83) is computed more effectively as

$$G_R(\boldsymbol{x},\boldsymbol{y}) = \frac{1}{\pi}\int_0^\infty \left(\frac{e^{-\sqrt{\xi^2-k^2}\,v_2}}{Z_\infty - \sqrt{\xi^2-k^2}} - \frac{2Z_\infty e^{-Z_\infty v_2}}{\xi_p^2-\xi^2} - \frac{e^{-\sqrt{\xi^2-k^2}\,v_2}}{\sqrt{\xi^2-k^2}} \right)\cos(\xi v_1)\,\mathrm{d}\xi$$
$$- \frac{iZ_\infty}{\xi_p}\,e^{-Z_\infty v_2}e^{i\xi_p|v_1|} + \frac{i}{2}H_0^{(1)}\big(k|\boldsymbol{y}-\bar{\boldsymbol{x}}|\big). \quad (3.92)$$

The expressions (3.87), (3.90), and (3.92) are likewise valid when $v_2 = 0$, which allows to evaluate the term G_B in (3.85).

f) Complete spatial Green's function

The desired complete spatial Green's function is finally obtained, as stated in (3.67), by adding the terms (3.70), (3.73), (3.74), and (3.81). It can be appreciated graphically in Figures 3.5 & 3.6 for $k = 1.2$, $Z_\infty = 1$, and $\boldsymbol{x} = (0, 2)$, and it is given explicitly by

$$G(\boldsymbol{x}, \boldsymbol{y}) = -\frac{i}{4} H_0^{(1)}\big(k|\boldsymbol{y} - \boldsymbol{x}|\big) + \frac{i}{4} H_0^{(1)}\big(k|\boldsymbol{y} - \bar{\boldsymbol{x}}|\big) - \frac{iZ_\infty}{\xi_p}\, e^{-Z_\infty v_2} \cos(\xi_p v_1) + \frac{ik}{2}\, e^{-Z_\infty v_2} \int_{-\infty}^{v_2} H_1^{(1)}\Big(k\sqrt{v_1^2 + \eta^2}\Big)\, \frac{\eta\, e^{Z_\infty \eta}}{\sqrt{v_1^2 + \eta^2}}\, \mathrm{d}\eta, \tag{3.93}$$

where we use the notation (3.76). The integral in (3.93) can be computed either as (3.83) or as (3.84), depending on wether $v_2 > 0$ or $v_2 < 0$. The involved Fourier integrals of the remaining term G_R are computed according to the expressions (3.87), (3.90), and (3.92).

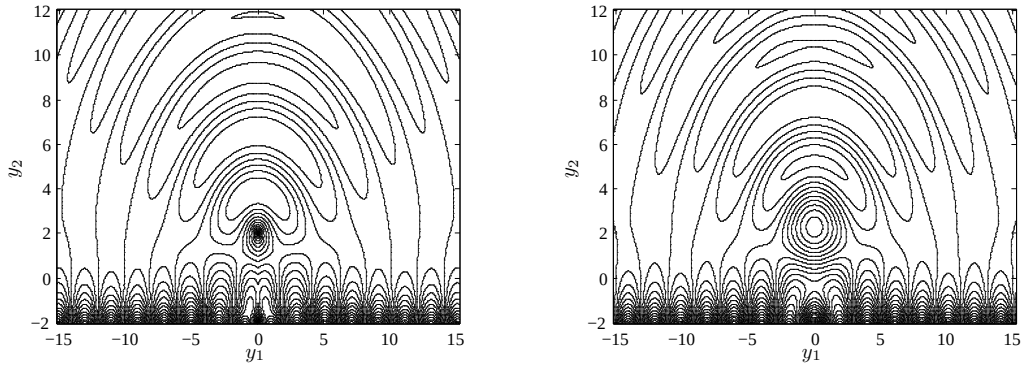

(a) Real part (b) Imaginary part

FIGURE 3.5. Contour plot of the complete spatial Green's function.

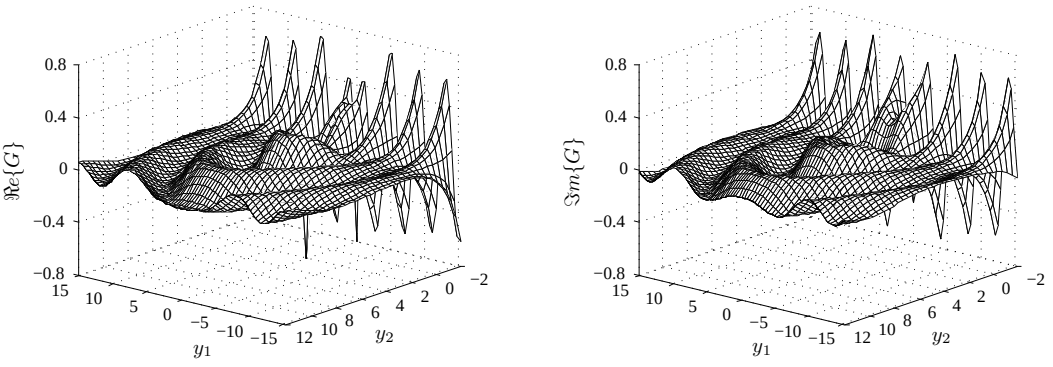

(a) Real part (b) Imaginary part

FIGURE 3.6. Oblique view of the complete spatial Green's function.

For the derivative of the Green's function with respect to the y_2-variable, it holds that

$$\frac{\partial G}{\partial y_2}(\boldsymbol{x},\boldsymbol{y}) = \frac{ik}{4}H_1^{(1)}\big(k|\boldsymbol{y}-\boldsymbol{x}|\big)\frac{y_2-x_2}{|\boldsymbol{y}-\boldsymbol{x}|} + \frac{ik}{4}H_1^{(1)}\big(k|\boldsymbol{y}-\bar{\boldsymbol{x}}|\big)\frac{v_2}{|\boldsymbol{y}-\bar{\boldsymbol{x}}|}$$
$$+ \frac{iZ_\infty^2}{\xi_p}\,e^{-Z_\infty v_2}\cos(\xi_p v_1) - \frac{ikZ_\infty}{2}\,e^{-Z_\infty v_2}\int_{-\infty}^{v_2} H_1^{(1)}\Big(k\sqrt{v_1^2+\eta^2}\Big)\,\frac{\eta\,e^{Z_\infty\eta}}{\sqrt{v_1^2+\eta^2}}\,\mathrm{d}\eta. \quad (3.94)$$

The integral in (3.94) is computed the same way as in (3.93). The derivative with respect to the y_1-variable, on the other hand, is given by

$$\frac{\partial G}{\partial y_1}(\boldsymbol{x},\boldsymbol{y}) = \frac{ik}{4}H_1^{(1)}\big(k|\boldsymbol{y}-\boldsymbol{x}|\big)\frac{v_1}{|\boldsymbol{y}-\boldsymbol{x}|} - \frac{ik}{4}H_1^{(1)}\big(k|\boldsymbol{y}-\bar{\boldsymbol{x}}|\big)\frac{v_1}{|\boldsymbol{y}-\bar{\boldsymbol{x}}|}$$
$$+ iZ_\infty e^{-Z_\infty v_2}\sin(\xi_p v_1) + \frac{ik^2}{2}\,e^{-Z_\infty v_2}\int_{-\infty}^{v_2} H_0^{(1)}\Big(k\sqrt{v_1^2+\eta^2}\Big)\,\frac{v_1^2}{v_1^2+\eta^2}\,e^{Z_\infty\eta}\,\mathrm{d}\eta$$
$$+ \frac{ik}{2}\,e^{-Z_\infty v_2}\int_{-\infty}^{v_2} H_1^{(1)}\Big(k\sqrt{v_1^2+\eta^2}\Big)\,\frac{\eta^2-v_1^2}{(v_1^2+\eta^2)^{3/2}}\,e^{Z_\infty\eta}\,\mathrm{d}\eta. \quad (3.95)$$

The integrals in (3.95) are related with the remaining term G_R and are computed respectively as the y_1-derivative of (3.84), (3.87), (3.90), and (3.92), e.g., the y_1-derivative of the Fourier integral (3.83) becomes

$$\frac{\partial G_R}{\partial y_1}(\boldsymbol{x},\boldsymbol{y}) = -\frac{1}{\pi}\int_0^\infty \frac{\xi\,e^{-\sqrt{\xi^2-k^2}\,v_2}}{Z_\infty-\sqrt{\xi^2-k^2}}\sin(\xi v_1)\,\mathrm{d}\xi. \quad (3.96)$$

The other cases are modified analogously.

3.3.5 Extension and properties

The half-plane Green's function can be extended in a locally analytic way towards the full-plane $\mathbb{R}^2$ in a straightforward and natural manner, just by considering the expression (3.93) valid for all $\boldsymbol{x},\boldsymbol{y}\in\mathbb{R}^2$, instead of just for $\mathbb{R}^2_+$. This extension possesses two singularities of logarithmic type at the points $\boldsymbol{x}$ and $\bar{\boldsymbol{x}}$, and is continuous otherwise. The behavior of these singularities is characterized by

$$G(\boldsymbol{x},\boldsymbol{y}) \sim \frac{1}{2\pi}\ln|\boldsymbol{y}-\boldsymbol{x}|, \qquad \boldsymbol{y}\longrightarrow\boldsymbol{x}, \quad (3.97)$$

$$G(\boldsymbol{x},\boldsymbol{y}) \sim \frac{1}{2\pi}\ln|\boldsymbol{y}-\bar{\boldsymbol{x}}|, \qquad \boldsymbol{y}\longrightarrow\bar{\boldsymbol{x}}. \quad (3.98)$$

For the y_1-derivative there appears a jump across the half-line $\Upsilon=\{y_1=x_1, y_2<-x_2\}$, due the effect of the analytic branch cut of the exponential integral functions, shown in Figure 3.7. We denote this jump by

$$J(\boldsymbol{x},\boldsymbol{y}) = \lim_{y_1\to x_1^+}\left\{\frac{\partial G}{\partial y_1}\right\} - \lim_{y_1\to x_1^-}\left\{\frac{\partial G}{\partial y_1}\right\} = \frac{\partial G}{\partial y_1^+}\bigg|_{y_1=x_1} - \frac{\partial G}{\partial y_1^-}\bigg|_{y_1=x_1}. \quad (3.99)$$

This jump across Υ is the same as for the Laplace equation in (2.104), since the involved singularities are the same, i.e., it has a value of

$$J(\boldsymbol{x},\boldsymbol{y}) = 2Z_\infty e^{-Z_\infty(y_2+x_2)}. \quad (3.100)$$

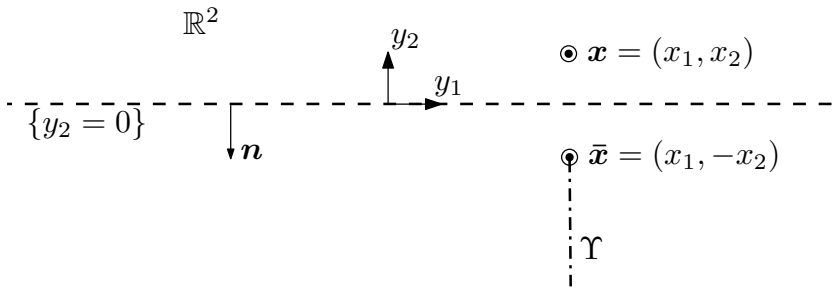

FIGURE 3.7. Domain of the extended Green's function.

We remark that the Green's function (3.93) itself and its y_2-derivative are continuous across the half-line Υ.

As long as $x_2 \neq 0$, it is clear that the impedance boundary condition in (3.20) continues to be homogeneous. Nonetheless, if the source point $\boldsymbol{x}$ lies on the half-plane's boundary, i.e., if $x_2 = 0$, then the boundary condition ceases to be homogeneous in the sense of distributions. This can be deduced from the expression (3.66) by verifying that

$$\lim_{y_2 \to 0^+} \left\{ \frac{\partial G}{\partial y_2}\big((x_1, 0), \boldsymbol{y}\big) + Z_\infty G\big((x_1, 0), \boldsymbol{y}\big) \right\} = \delta_{x_1}(y_1). \tag{3.101}$$

Since the impedance boundary condition holds only on $\{y_2 = 0\}$, therefore the right-hand side of (3.101) can be also expressed by

$$\delta_{x_1}(y_1) = \frac{1}{2}\delta_{\boldsymbol{x}}(\boldsymbol{y}) + \frac{1}{2}\delta_{\bar{\boldsymbol{x}}}(\boldsymbol{y}), \tag{3.102}$$

which illustrates more clearly the contribution of each logarithmic singularity to the Dirac mass in the boundary condition.

It can be seen now that the Green's function extended in the abovementioned way satisfies, for $\boldsymbol{x} \in \mathbb{R}^2$, in the sense of distributions, and instead of (3.20), the problem

$$\begin{cases} \text{Find } G(\boldsymbol{x}, \cdot) : \mathbb{R}^2 \to \mathbb{C} \text{ such that} \\ \Delta_{\boldsymbol{y}} G(\boldsymbol{x}, \boldsymbol{y}) + k^2 G(\boldsymbol{x}, \boldsymbol{y}) = \delta_{\boldsymbol{x}}(\boldsymbol{y}) + \delta_{\bar{\boldsymbol{x}}}(\boldsymbol{y}) + J(\boldsymbol{x}, \boldsymbol{y})\delta_\Upsilon(\boldsymbol{y}) \quad \text{in } \mathcal{D}'(\mathbb{R}^2), \\ \dfrac{\partial G}{\partial y_2}(\boldsymbol{x}, \boldsymbol{y}) + Z_\infty G(\boldsymbol{x}, \boldsymbol{y}) = \dfrac{1}{2}\delta_{\boldsymbol{x}}(\boldsymbol{y}) + \dfrac{1}{2}\delta_{\bar{\boldsymbol{x}}}(\boldsymbol{y}) \quad \text{on } \{y_2 = 0\}, \\ + \text{ Outgoing radiation condition for } \boldsymbol{y} \in \mathbb{R}^2_+ \text{ as } |\boldsymbol{y}| \to \infty, \end{cases} \tag{3.103}$$

where δ_Υ denotes a Dirac mass distribution along the Υ-curve. We retrieve thus the known result that for an impedance boundary condition the image of a point source is a point source plus a half-line of sources with exponentially increasing strengths in the lower half-plane, and which extends from the image point source towards infinity along the half-plane's normal direction (cf. Keller 1979, who refers to decreasing strengths when dealing with the opposite half-plane).

We note that the half-plane Green's function (3.93) is symmetric in the sense that

$$G(\boldsymbol{x}, \boldsymbol{y}) = G(\boldsymbol{y}, \boldsymbol{x}) \qquad \forall \boldsymbol{x}, \boldsymbol{y} \in \mathbb{R}^2, \tag{3.104}$$

and it fulfills similarly

$$\nabla_{\boldsymbol{y}} G(\boldsymbol{x},\boldsymbol{y}) = \nabla_{\boldsymbol{y}} G(\boldsymbol{y},\boldsymbol{x}) \qquad \text{and} \qquad \nabla_{\boldsymbol{x}} G(\boldsymbol{x},\boldsymbol{y}) = \nabla_{\boldsymbol{x}} G(\boldsymbol{y},\boldsymbol{x}). \tag{3.105}$$

Another property is that we retrieve the special case (3.23) of a homogenous Dirichlet boundary condition in $\mathbb{R}^2_+$ when $Z_\infty \to \infty$. Likewise, we retrieve the special case (3.25) of a homogenous Neumann boundary condition in $\mathbb{R}^2_+$ when $Z_\infty \to 0$, except for an additive constant due the extra term (3.74) that can be disregarded.

At last, we observe that the expression for the Green's function (3.93) is still valid if a complex wave number $k \in \mathbb{C}$, such that $\mathfrak{Im}\{k\} > 0$ and $\mathfrak{Re}\{k\} \geq 0$, and a complex impedance $Z_\infty \in \mathbb{C}$, such that $\mathfrak{Im}\{Z_\infty\} > 0$ and $\mathfrak{Re}\{Z_\infty\} \geq 0$, are used, which holds also for its derivatives. The logarithms, though, have to be interpreted analogously as in (2.111) and (2.112) to avoid an undesired behavior in the lower half-plane, i.e., as

$$\ln\big(Z_\infty v_2 - i\xi_p v_1\big) = \ln\big(v_2 - i v_1 \xi_p / Z_\infty\big) + \ln(Z_\infty), \tag{3.106}$$

$$\ln\big(Z_\infty v_2 + i\xi_p v_1\big) = \ln\big(v_2 + i v_1 \xi_p / Z_\infty\big) + \ln(Z_\infty), \tag{3.107}$$

where the principal value is considered for the logarithms on the right-hand side.

3.4 Far field of the Green's function

3.4.1 Decomposition of the far field

The far field of the Green's function, which we denote by G^{ff}, describes its asymptotic behavior at infinity, i.e., when $|\boldsymbol{x}| \to \infty$ and assuming that $\boldsymbol{y}$ is fixed. For this purpose, the terms of highest order at infinity are searched. Likewise as done for the radiation condition, the far field can be decomposed into two parts, each acting on a different region as shown in Figure 3.2. The first part, denoted by G^{ff}_V, is linked with the volume waves, and acts in the interior of the half-plane while vanishing near its boundary. The second part, denoted by G^{ff}_S, is associated with surface waves that propagate along the boundary towards infinity, which decay exponentially towards the half-plane's interior. We have thus that

$$G^{ff} = G^{ff}_V + G^{ff}_S. \tag{3.108}$$

3.4.2 Volume waves in the far field

The volume waves in the far field act only in the interior of the half-plane and are related to the terms of the Hankel functions in (3.93), and also to the asymptotic behavior as $x_2 \to \infty$ of the regular part. The behavior of the volume waves can be obtained by applying the stationary phase technique on the integrals in (3.66), as performed by Durán, Muga & Nédélec (2005*a*, 2006). This technique gives an expression for the leading asymptotic behavior of highly oscillating integrals in the form of

$$I(\lambda) = \int_a^b f(s) e^{i\lambda\phi(s)}\,\mathrm{d}s, \tag{3.109}$$

as $\lambda \to \infty$ along the positive real axis, where $\phi(s)$ is a regular real function, where $|f(s)|$ is integrable, and where the real integration limits a and b may be unbounded. Further

references on the stationary phase technique are Bender & Orszag (1978), Dettman (1984), Evans (1998), and Watson (1944). Integrals in the form of (3.109) are called generalized Fourier integrals. They tend towards zero very rapidly with λ, except at the so-called stationary points for which the derivative of the phase becomes zero, where the integrand vanishes less rapidly. If s_0 is such a stationary point, i.e., if $\phi'(s_0) = 0$, and if $\phi''(s_0) > 0$, then the main asymptotic contribution of the integral (3.109) is given by

$$I(\lambda) \sim e^{i\pi/4} \sqrt{\frac{2\pi}{\lambda \phi''(s_0)}}\, f(s_0) e^{i\lambda\phi(s_0)}. \tag{3.110}$$

Moreover, the residue is uniformly bounded by $C\lambda^{-3/2}$ for some constant $C > 0$ if the point s_0 is not an end-point of the integration domain.

The asymptotic behavior of the volume waves is related with the terms in (3.66) which do not decrease exponentially as $x_2 \to \infty$, i.e., with the integral terms for which $\sqrt{\xi^2 - k^2}$ is purely imaginary, which occurs when $|\xi| < k$. Hence, as $x_2 \to \infty$ it holds that

$$\begin{aligned} G(\boldsymbol{x}, \boldsymbol{y}) \sim & -\frac{1}{4\pi} \int_{|\xi|<k} \frac{e^{-\sqrt{\xi^2-k^2}\,|x_2-y_2|}}{\sqrt{\xi^2-k^2}}\, e^{-i\xi(x_1-y_1)} \mathrm{d}\xi \\ & + \frac{1}{4\pi} \int_{|\xi|<k} \left(\frac{Z_\infty + \sqrt{\xi^2-k^2}}{Z_\infty - \sqrt{\xi^2-k^2}} \right) \frac{e^{-\sqrt{\xi^2-k^2}\,(x_2+y_2)}}{\sqrt{\xi^2-k^2}}\, e^{-i\xi(x_1-y_1)} \mathrm{d}\xi. \end{aligned} \tag{3.111}$$

By using the change of variable $\xi = -k\cos\psi$, for $0 \le \psi \le \pi$, we obtain that

$$G(\boldsymbol{x}, \boldsymbol{y}) \sim \frac{i}{4\pi} \int_0^\pi \left(-1 + \frac{Z_\infty - ik\sin\psi}{Z_\infty + ik\sin\psi}\, e^{2iky_2\sin\psi} \right) e^{ik|\boldsymbol{x}-\boldsymbol{y}|\cos(\psi-\alpha)} \mathrm{d}\psi, \tag{3.112}$$

where α is such that

$$\cos\alpha = \frac{x_1 - y_1}{|\boldsymbol{x}-\boldsymbol{y}|} \qquad \text{and} \qquad \sin\alpha = \frac{x_2 - y_2}{|\boldsymbol{x}-\boldsymbol{y}|}. \tag{3.113}$$

The phase $\phi(\psi) = k\cos(\psi - \alpha)$ has only one stationary point, namely $\psi = \alpha$, which lies inside the interval $(0, \pi)$. Hence, from (3.110) we obtain that

$$G(\boldsymbol{x}, \boldsymbol{y}) \sim \frac{e^{i\pi/4}}{\sqrt{8\pi k}} \frac{e^{ik|\boldsymbol{x}-\boldsymbol{y}|}}{\sqrt{|\boldsymbol{x}-\boldsymbol{y}|}} \left(-1 + \frac{Z_\infty - ik\sin\alpha}{Z_\infty + ik\sin\alpha}\, e^{2iky_2\sin\alpha} \right), \tag{3.114}$$

Due the asymptotic behavior (A.139) of the Hankel function $H_0^{(1)}$, it holds that

$$H_0^{(1)}\big(k|\boldsymbol{x}-\boldsymbol{y}|\big) \sim e^{-i\pi/4} \sqrt{\frac{2}{\pi k}} \frac{e^{ik|\boldsymbol{x}-\boldsymbol{y}|}}{\sqrt{|\boldsymbol{x}-\boldsymbol{y}|}}, \tag{3.115}$$

$$H_0^{(1)}\big(k|\boldsymbol{x}-\bar{\boldsymbol{y}}|\big) \sim e^{-i\pi/4} \sqrt{\frac{2}{\pi k}} \frac{e^{ik|\boldsymbol{x}-\bar{\boldsymbol{y}}|}}{\sqrt{|\boldsymbol{x}-\bar{\boldsymbol{y}}|}}, \tag{3.116}$$

as $|\boldsymbol{x}| \to \infty$, where $\bar{\boldsymbol{y}} = (y_1, -y_2)$. Since $|\boldsymbol{x}-\bar{\boldsymbol{y}}| \sim |\boldsymbol{x}-\boldsymbol{y}|$ as $x_2 \to \infty$, this implies that the asymptotic behavior (3.114) can be equivalently stated as

$$G(\boldsymbol{x}, \boldsymbol{y}) \sim -\frac{i}{4} H_0^{(1)}\big(k|\boldsymbol{x}-\boldsymbol{y}|\big) + \frac{i}{4} \left(\frac{Z_\infty - ik\sin\alpha}{Z_\infty + ik\sin\alpha} \right) H_0^{(1)}\big(k|\boldsymbol{x}-\bar{\boldsymbol{y}}|\big). \tag{3.117}$$

By performing Taylor expansions, as in (C.37) and (C.38), we have that

$$\frac{e^{ik|\boldsymbol{x}-\boldsymbol{y}|}}{\sqrt{|\boldsymbol{x}-\boldsymbol{y}|}} = \frac{e^{ik|\boldsymbol{x}|}}{\sqrt{|\boldsymbol{x}|}}\, e^{-ik\boldsymbol{y}\cdot\boldsymbol{x}/|\boldsymbol{x}|} \left(1 + \mathcal{O}\Big(\frac{1}{|\boldsymbol{x}|}\Big)\right), \tag{3.118}$$

$$\frac{e^{ik|\boldsymbol{x}-\bar{\boldsymbol{y}}|}}{\sqrt{|\boldsymbol{x}-\bar{\boldsymbol{y}}|}} = \frac{e^{ik|\boldsymbol{x}|}}{\sqrt{|\boldsymbol{x}|}}\, e^{-ik\bar{\boldsymbol{y}}\cdot\boldsymbol{x}/|\boldsymbol{x}|} \left(1 + \mathcal{O}\Big(\frac{1}{|\boldsymbol{x}|}\Big)\right). \tag{3.119}$$

We express the point $\boldsymbol{x}$ as $\boldsymbol{x} = |\boldsymbol{x}|\,\hat{\boldsymbol{x}}$, being $\hat{\boldsymbol{x}} = (\cos\theta, \sin\theta)$ a unitary vector. Similar Taylor expansions as before yield that

$$\frac{Z_\infty - ik\sin\alpha}{Z_\infty + ik\sin\alpha} = \frac{Z_\infty - ik\sin\theta}{Z_\infty + ik\sin\theta} \left(1 + \mathcal{O}\Big(\frac{1}{|\boldsymbol{x}|}\Big)\right). \tag{3.120}$$

The volume-wave behavior of the Green's function, from (3.114) and due (3.118), (3.119), and (3.120), becomes thus

$$G_V^{ff}(\boldsymbol{x},\boldsymbol{y}) = \frac{e^{i\pi/4}}{\sqrt{8\pi k}} \frac{e^{ik|\boldsymbol{x}|}}{\sqrt{|\boldsymbol{x}|}}\, e^{-ik\hat{\boldsymbol{x}}\cdot\boldsymbol{y}} \left(-1 + \frac{Z_\infty - ik\sin\theta}{Z_\infty + ik\sin\theta}\, e^{2iky_2\sin\theta}\right), \tag{3.121}$$

and its gradient with respect to $\boldsymbol{y}$ is given by

$$\nabla_{\boldsymbol{y}} G_V^{ff}(\boldsymbol{x},\boldsymbol{y}) = e^{-i\pi/4}\sqrt{\frac{k}{8\pi}}\, \frac{e^{ik|\boldsymbol{x}|}}{\sqrt{|\boldsymbol{x}|}}\, e^{-ik\hat{\boldsymbol{x}}\cdot\boldsymbol{y}} \left(-\hat{\boldsymbol{x}} + \frac{Z_\infty - ik\sin\theta}{Z_\infty + ik\sin\theta}\, e^{2iky_2\sin\theta} \begin{bmatrix} \cos\theta \\ -\sin\theta \end{bmatrix}\right). \tag{3.122}$$

3.4.3 Surface waves in the far field

An expression for the surface waves in the far field can be obtained by studying the residues of the poles of the spectral Green's function, which determine entirely their asymptotic behavior. We already computed the inverse Fourier transform of these residues in (3.55), using the residue theorem of Cauchy and the limiting absorption principle. This implies that the Green's function behaves asymptotically, when $|x_1| \to \infty$, as

$$G(\boldsymbol{x},\boldsymbol{y}) \sim -\frac{iZ_\infty}{\xi_p}\, e^{-Z_\infty(x_2+y_2)} e^{i\xi_p|x_1-y_1|}, \tag{3.123}$$

where $\xi_p = \sqrt{Z_\infty^2 + k^2}$. More detailed computations can be found in Durán, Muga & Nédélec (2005*a*, 2006). Similarly as in (C.36), we can use Taylor expansions to obtain

$$|x_1 - y_1| = |x_1| - y_1 \operatorname{sign} x_1 + \mathcal{O}\Big(\frac{1}{|x_1|}\Big). \tag{3.124}$$

Therefore, as for (C.38), we have that

$$e^{i\xi_p|x_1-y_1|} = e^{i\xi_p|x_1|} e^{-i\xi_p y_1 \operatorname{sign} x_1} \left(1 + \mathcal{O}\Big(\frac{1}{|x_1|}\Big)\right). \tag{3.125}$$

The surface-wave behavior of the Green's function, due (3.123) and (3.125), becomes thus

$$G_S^{ff}(\boldsymbol{x},\boldsymbol{y}) = -\frac{iZ_\infty}{\xi_p}\, e^{-Z_\infty x_2} e^{i\xi_p|x_1|} e^{-Z_\infty y_2} e^{-i\xi_p y_1 \operatorname{sign} x_1}, \tag{3.126}$$

and its gradient with respect to $\boldsymbol{y}$ is given by

$$\nabla_{\boldsymbol{y}} G_S^{ff}(\boldsymbol{x},\boldsymbol{y}) = -\frac{Z_\infty}{\xi_p}\, e^{-Z_\infty x_2} e^{i\xi_p|x_1|} e^{-Z_\infty y_2} e^{-i\xi_p y_1 \operatorname{sign} x_1} \begin{bmatrix} \xi_p \operatorname{sign} x_1 \\ -iZ_\infty \end{bmatrix}. \tag{3.127}$$

3.4.4 Complete far field of the Green's function

On the whole, the asymptotic behavior of the Green's function as $|\boldsymbol{x}| \to \infty$ can be characterized through the addition of (3.117) and (3.123), namely

$$\begin{aligned} G(\boldsymbol{x},\boldsymbol{y}) \sim & -\frac{i}{4} H_0^{(1)}\big(k|\boldsymbol{x}-\boldsymbol{y}|\big) + \frac{i}{4}\left(\frac{Z_\infty - ik\sin\alpha}{Z_\infty + ik\sin\alpha}\right) H_0^{(1)}\big(k|\boldsymbol{x}-\bar{\boldsymbol{y}}|\big) \\ & - \frac{iZ_\infty}{\xi_p}\, e^{-Z_\infty(x_2+y_2)} e^{i\xi_p|x_1-y_1|}. \end{aligned} \tag{3.128}$$

Consequently, the complete far field of the Green's function, due (3.108), is given by the addition of (3.121) and (3.126), i.e., by

$$\begin{aligned} G^{ff}(\boldsymbol{x},\boldsymbol{y}) = & \frac{e^{i\pi/4}}{\sqrt{8\pi k}} \frac{e^{ik|\boldsymbol{x}|}}{\sqrt{|\boldsymbol{x}|}}\, e^{-ik\hat{\boldsymbol{x}}\cdot\boldsymbol{y}} \left(-1 + \frac{Z_\infty - ik\sin\theta}{Z_\infty + ik\sin\theta}\, e^{2iky_2\sin\theta}\right) \\ & - \frac{iZ_\infty}{\xi_p}\, e^{-Z_\infty x_2} e^{i\xi_p|x_1|} e^{-Z_\infty y_2} e^{-i\xi_p y_1 \operatorname{sign} x_1}. \end{aligned} \tag{3.129}$$

Its derivative with respect to $\boldsymbol{y}$ is likewise given by the addition of (3.122) and (3.127).

It is this far field (3.129) that justifies the radiation condition (3.21) when exchanging the roles of $\boldsymbol{x}$ and $\boldsymbol{y}$. When the first term in (3.129) dominates, i.e., the volume waves (3.121), then it is the first expression in (3.21) that matters. Conversely, when the second term in (3.129) dominates, i.e., the surface waves (3.126), then the second expression in (3.21) is the one that holds. The interface between both asymptotic behaviors can be determined by equating the amplitudes of the two terms in (3.129), i.e., by searching values of $\boldsymbol{x}$ at infinity such that

$$\frac{1}{\sqrt{8\pi k|\boldsymbol{x}|}} = \frac{Z_\infty}{\xi_p}\, e^{-Z_\infty x_2}, \tag{3.130}$$

where the values of $\boldsymbol{y}$ can be neglected, since they remain relatively near the origin. By taking the logarithm in (3.130) and perturbing somewhat the result so as to avoid a singular behavior at the origin, we obtain finally that this interface is described by

$$x_2 = \frac{1}{Z_\infty} \ln\left(1 + \frac{8\pi k Z_\infty^2}{Z_\infty^2 + k^2}|\boldsymbol{x}|\right). \tag{3.131}$$

We remark that the asymptotic behavior (3.128) of the Green's function and the expression (3.129) of its complete far field do no longer hold if a complex impedance $Z_\infty \in \mathbb{C}$ such that $\mathfrak{Im}\{Z_\infty\} > 0$ and $\mathfrak{Re}\{Z_\infty\} \geq 0$ is used, specifically the parts (3.123) and (3.126) linked with the surface waves. A careful inspection shows that in this case the surface-wave

behavior of the Green's function, as $|x_1| \to \infty$, decreases exponentially and is given by

$$G(\boldsymbol{x},\boldsymbol{y}) \sim \begin{cases} -\dfrac{iZ_\infty}{\xi_p}\, e^{-|Z_\infty|(x_2+y_2)} e^{i\xi_p|x_1-y_1|} & \text{if } (x_2+y_2) > 0, \\ -\dfrac{iZ_\infty}{\xi_p}\, e^{-Z_\infty(x_2+y_2)} e^{i\xi_p|x_1-y_1|} & \text{if } (x_2+y_2) \leq 0. \end{cases} \tag{3.132}$$

Therefore the surface-wave part of the far field can be now expressed as

$$G_S^{ff}(\boldsymbol{x},\boldsymbol{y}) = \begin{cases} -\dfrac{iZ_\infty}{\xi_p}\, e^{-|Z_\infty|\, x_2} e^{i\xi_p|x_1|} e^{-|Z_\infty|\, y_2} e^{-i\xi_p y_1 \operatorname{sign} x_1} & \text{if } x_2 > 0, \\ -\dfrac{iZ_\infty}{\xi_p}\, e^{-Z_\infty x_2} e^{i\xi_p|x_1|} e^{-Z_\infty y_2} e^{-i\xi_p y_1 \operatorname{sign} x_1} & \text{if } x_2 \leq 0. \end{cases} \tag{3.133}$$

The volume-waves part (3.117) and its far-field expression (3.121), on the other hand, remain the same when we use a complex impedance. We remark further that if a complex impedance or a complex wave number are taken into account, then the part of the surface waves of the outgoing radiation condition is redundant, and only the volume-waves part is required, i.e., only the first two expressions in (3.21), but now holding for $y_2 > 0$.

3.5 Numerical evaluation of the Green's function

For the numerical evaluation of the Green's function, we separate the plane $\mathbb{R}^2$ into three regions: an upper near field, a lower near field, and a far field. The near field is given by the region $|k|\,|\boldsymbol{v}| \leq 24$ and the far field encompasses $|k|\,|\boldsymbol{v}| > 24$, being $\boldsymbol{v} = \boldsymbol{y} - \bar{\boldsymbol{x}}$.

The upper near field considers $v_2 \geq 0$ and the lower near field $v_2 < 0$. In the upper near field, when $|Z_\infty| \geq |k|$ and $2|\xi_p| \geq |Z_\infty|$, the Green's function is computed by using the expression (3.87). The second condition is required, since the spectral part of (3.87) becomes slowly decreasing when $|\xi_p|$ is very small compared with $|Z_\infty|$, i.e., in the case when $Z_\infty \approx ik$. When $|Z_\infty| < |k|$ or when $2|\xi_p| < |Z_\infty|$, the Green's function is evaluated in the upper near field using (3.90) and (3.92), depending on wether $\arg(k) \leq \pi/4$ or $\arg(k) > \pi/4$, respectively. In the lower near field, on the other hand, we use the expression (3.84) to compute the Green's function, where the term G_B is computed analogously as the Green's function in the upper near field, but considering $v_2 = 0$. The numerical integration of the Fourier integrals is performed by means of a trapezoidal rule, discretizing the spectral variable ξ into $\xi_j = j\Delta\xi$ for $j = 0, \ldots, M$, where

$$\Delta\xi = \frac{2\pi|k|}{12 \cdot 24} \qquad \text{and} \qquad \xi_M = M\Delta\xi \approx |k|\Big(2 + 8\, e^{-4v_2|Z_\infty|/|k|}\Big), \tag{3.134}$$

taking thus at least 12 samples per oscillation and increasing the size of the integration interval as v_2 approaches to zero. This discretization contains all the relevant information for an accurate numerical integration.

In the far field, the Green's function can be computed either by using (3.128) or by considering the exponential integral functions for the surface-wave terms, i.e., by considering

that as $|\boldsymbol{x}| \to \infty$ it holds that

$$G(\boldsymbol{x},\boldsymbol{y}) \sim -\frac{i}{4}H_0^{(1)}\big(k|\boldsymbol{x}-\boldsymbol{y}|\big) + \frac{i}{4}\left(\frac{Z_\infty - ik\sin\alpha}{Z_\infty + ik\sin\alpha}\right)H_0^{(1)}\big(k|\boldsymbol{x}-\bar{\boldsymbol{y}}|\big)$$
$$+ \frac{Z_\infty}{2\pi\xi_p}\,e^{-Z_\infty v_2}\Big\{e^{i\xi_p v_1}\,\mathrm{Ei}(Z_\infty v_2 - i\xi_p v_1) + e^{-i\xi_p v_1}\,\mathrm{Ei}(Z_\infty v_2 + i\xi_p v_1)\Big\}$$
$$- \frac{iZ_\infty}{\xi_p}\,e^{-Z_\infty v_2}\cos(\xi_p v_1). \tag{3.135}$$

The Bessel functions can be evaluated either by using the software based on the technical report by Morris (1993) or the subroutines described in Amos (1986, 1995). The exponential integral function for complex arguments can be computed by using the algorithm developed by Amos (1980, 1990*a*,*b*) or the software based on the technical report by Morris (1993), taking care with the definition of the analytic branch cuts. Further references are listed in Lozier & Olver (1994). The biggest numerical error, excepting the singularity-distribution along the half-line Υ, is committed near the boundaries of the three described regions, and is more or less of order $6\,|k|\,/\,|Z_\infty|\cdot 10^{-3}$.

3.6 Integral representation and equation

3.6.1 Integral representation

We are interested in expressing the solution u of the direct scattering problem (3.13) by means of an integral representation formula over the perturbed portion of the boundary Γ_p. For this purpose, we extend this solution by zero towards the complementary domain Ω_c, analogously as done in (C.107). We define by $\Omega_{R,\varepsilon}$ the domain Ω_e without the ball B_ε of radius $\varepsilon > 0$ centered at the point $\boldsymbol{x} \in \Omega_e$, and truncated at infinity by the ball B_R of radius $R > 0$ centered at the origin. We consider that the ball B_ε is entirely contained in Ω_e. Therefore, as shown in Figure 3.8, we have that

$$\Omega_{R,\varepsilon} = \big(\Omega_e \cap B_R\big) \setminus \overline{B_\varepsilon}, \tag{3.136}$$

where

$$B_R = \{\boldsymbol{y} \in \mathbb{R}^2 :\, |\boldsymbol{y}| < R\} \qquad \text{and} \qquad B_\varepsilon = \{\boldsymbol{y} \in \Omega_e :\, |\boldsymbol{y}-\boldsymbol{x}| < \varepsilon\}. \tag{3.137}$$

We consider similarly, inside Ω_e, the boundaries of the balls

$$S_R^+ = \{\boldsymbol{y} \in \mathbb{R}^2_+ :\, |\boldsymbol{y}| = R\} \qquad \text{and} \qquad S_\varepsilon = \{\boldsymbol{y} \in \Omega_e :\, |\boldsymbol{y}-\boldsymbol{x}| = \varepsilon\}. \tag{3.138}$$

We separate furthermore the boundary as $\Gamma = \Gamma_0 \cup \Gamma_+$, where

$$\Gamma_0 = \{\boldsymbol{y} \in \Gamma :\, y_2 = 0\} \qquad \text{and} \qquad \Gamma_+ = \{\boldsymbol{y} \in \Gamma :\, y_2 > 0\}. \tag{3.139}$$

The boundary Γ is likewise truncated at infinity by the ball B_R, namely

$$\Gamma_R = \Gamma \cap B_R = \Gamma_0^R \cup \Gamma_+ = \Gamma_\infty^R \cup \Gamma_p, \tag{3.140}$$

where

$$\Gamma_0^R = \Gamma_0 \cap B_R \qquad \text{and} \qquad \Gamma_\infty^R = \Gamma_\infty \cap B_R. \tag{3.141}$$

The idea is to retrieve the domain Ω_e and the boundary Γ at the end when the limits $R \to \infty$ and $\varepsilon \to 0$ are taken for the truncated domain $\Omega_{R,\varepsilon}$ and the truncated boundary Γ_R.

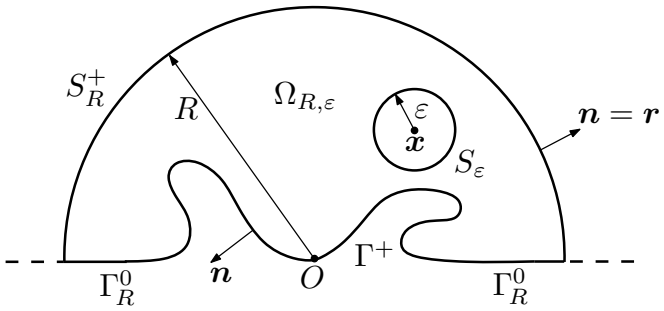

FIGURE 3.8. Truncated domain $\Omega_{R,\varepsilon}$ for $\boldsymbol{x} \in \Omega_e$.

We apply now Green's second integral theorem (A.613) to the functions u and $G(\boldsymbol{x}, \cdot)$ in the bounded domain $\Omega_{R,\varepsilon}$, by subtracting their respective Helmholtz equations, yielding

$$\begin{aligned} 0 &= \int_{\Omega_{R,\varepsilon}} \big(u(\boldsymbol{y})\Delta_{\boldsymbol{y}} G(\boldsymbol{x},\boldsymbol{y}) - G(\boldsymbol{x},\boldsymbol{y})\Delta u(\boldsymbol{y})\big)\mathrm{d}\boldsymbol{y} \\ &= \int_{S_R^+} \left(u(\boldsymbol{y})\frac{\partial G}{\partial r_{\boldsymbol{y}}}(\boldsymbol{x},\boldsymbol{y}) - G(\boldsymbol{x},\boldsymbol{y})\frac{\partial u}{\partial r}(\boldsymbol{y})\right)\mathrm{d}\gamma(\boldsymbol{y}) \\ &\quad - \int_{S_\varepsilon} \left(u(\boldsymbol{y})\frac{\partial G}{\partial r_{\boldsymbol{y}}}(\boldsymbol{x},\boldsymbol{y}) - G(\boldsymbol{x},\boldsymbol{y})\frac{\partial u}{\partial r}(\boldsymbol{y})\right)\mathrm{d}\gamma(\boldsymbol{y}) \\ &\quad + \int_{\Gamma_R} \left(u(\boldsymbol{y})\frac{\partial G}{\partial n_{\boldsymbol{y}}}(\boldsymbol{x},\boldsymbol{y}) - G(\boldsymbol{x},\boldsymbol{y})\frac{\partial u}{\partial n}(\boldsymbol{y})\right)\mathrm{d}\gamma(\boldsymbol{y}). \end{aligned} \tag{3.142}$$

The integral on S_R^+ can be rewritten as

$$\begin{aligned} &\int_{S_R^2} \left[u(\boldsymbol{y})\left(\frac{\partial G}{\partial r_{\boldsymbol{y}}}(\boldsymbol{x},\boldsymbol{y}) - iZ_\infty G(\boldsymbol{x},\boldsymbol{y})\right) - G(\boldsymbol{x},\boldsymbol{y})\left(\frac{\partial u}{\partial r}(\boldsymbol{y}) - iZ_\infty u(\boldsymbol{y})\right)\right]\mathrm{d}\gamma(\boldsymbol{y}) \\ &+ \int_{S_R^1} \left[u(\boldsymbol{y})\left(\frac{\partial G}{\partial r_{\boldsymbol{y}}}(\boldsymbol{x},\boldsymbol{y}) - ikG(\boldsymbol{x},\boldsymbol{y})\right) - G(\boldsymbol{x},\boldsymbol{y})\left(\frac{\partial u}{\partial r}(\boldsymbol{y}) - iku(\boldsymbol{y})\right)\right]\mathrm{d}\gamma(\boldsymbol{y}), \end{aligned} \tag{3.143}$$

which for R large enough and due the radiation condition (3.6) tends to zero, since

$$\left|\int_{S_R^2} u(\boldsymbol{y})\left(\frac{\partial G}{\partial r_{\boldsymbol{y}}}(\boldsymbol{x},\boldsymbol{y}) - i\sqrt{Z_\infty^2 + k^2}\, G(\boldsymbol{x},\boldsymbol{y})\right)\mathrm{d}\gamma(\boldsymbol{y})\right| \leq \frac{C}{R}\ln R, \tag{3.144}$$

$$\left|\int_{S_R^2} G(\boldsymbol{x},\boldsymbol{y})\left(\frac{\partial u}{\partial r}(\boldsymbol{y}) - i\sqrt{Z_\infty^2 + k^2}\, u(\boldsymbol{y})\right)\mathrm{d}\gamma(\boldsymbol{y})\right| \leq \frac{C}{R}\ln R, \tag{3.145}$$

and

$$\left|\int_{S_R^1} u(\boldsymbol{y})\left(\frac{\partial G}{\partial r_{\boldsymbol{y}}}(\boldsymbol{x},\boldsymbol{y}) - ikG(\boldsymbol{x},\boldsymbol{y})\right)\mathrm{d}\gamma(\boldsymbol{y})\right| \leq \frac{C}{\sqrt{R}}, \tag{3.146}$$

$$\left| \int_{S_R^1} G(\boldsymbol{x},\boldsymbol{y}) \left(\frac{\partial u}{\partial r}(\boldsymbol{y}) - iku(\boldsymbol{y}) \right) \mathrm{d}\gamma(\boldsymbol{y}) \right| \leq \frac{C}{\sqrt{R}}, \tag{3.147}$$

for some constants $C > 0$. If the function u is regular enough in the ball B_ε, then the second term of the integral on S_ε in (3.142), when $\varepsilon \to 0$ and due (3.97), is bounded by

$$\left| \int_{S_\varepsilon} G(\boldsymbol{x},\boldsymbol{y}) \frac{\partial u}{\partial r}(\boldsymbol{y}) \, \mathrm{d}\gamma(\boldsymbol{y}) \right| \leq C\varepsilon \ln \varepsilon \sup_{\boldsymbol{y}\in B_\varepsilon} \left| \frac{\partial u}{\partial r}(\boldsymbol{y}) \right|, \tag{3.148}$$

for some constant $C > 0$ and tends to zero. The regularity of u can be specified afterwards once the integral representation has been determined and generalized by means of density arguments. The first integral term on S_ε can be decomposed as

$$\begin{aligned} \int_{S_\varepsilon} u(\boldsymbol{y}) \frac{\partial G}{\partial r_{\boldsymbol{y}}}(\boldsymbol{x},\boldsymbol{y}) \, \mathrm{d}\gamma(\boldsymbol{y}) &= u(\boldsymbol{x}) \int_{S_\varepsilon} \frac{\partial G}{\partial r_{\boldsymbol{y}}}(\boldsymbol{x},\boldsymbol{y}) \, \mathrm{d}\gamma(\boldsymbol{y}) \\ &\quad + \int_{S_\varepsilon} \frac{\partial G}{\partial r_{\boldsymbol{y}}}(\boldsymbol{x},\boldsymbol{y}) \big(u(\boldsymbol{y}) - u(\boldsymbol{x}) \big) \, \mathrm{d}\gamma(\boldsymbol{y}), \end{aligned} \tag{3.149}$$

For the first term in the right-hand side of (3.149), by considering (3.97) we have that

$$\int_{S_\varepsilon} \frac{\partial G}{\partial r_{\boldsymbol{y}}}(\boldsymbol{x},\boldsymbol{y}) \, \mathrm{d}\gamma(\boldsymbol{y}) \quad \xrightarrow[\varepsilon\to 0]{} \quad 1, \tag{3.150}$$

while the second term is bounded by

$$\left| \int_{S_\varepsilon} \big(u(\boldsymbol{y}) - u(\boldsymbol{x}) \big) \frac{\partial G}{\partial r_{\boldsymbol{y}}}(\boldsymbol{x},\boldsymbol{y}) \, \mathrm{d}\gamma(\boldsymbol{y}) \right| \leq \sup_{\boldsymbol{y}\in B_\varepsilon} |u(\boldsymbol{y}) - u(\boldsymbol{x})|, \tag{3.151}$$

which tends towards zero when $\varepsilon \to 0$. Finally, due the impedance boundary condition (3.4) and since the support of f_z vanishes on Γ_∞, the term on Γ_R in (3.142) can be decomposed as

$$\begin{aligned} &\int_{\Gamma_p} \left(\frac{\partial G}{\partial n_{\boldsymbol{y}}}(\boldsymbol{x},\boldsymbol{y}) - Z(\boldsymbol{y}) G(\boldsymbol{x},\boldsymbol{y}) \right) u(\boldsymbol{y}) \, \mathrm{d}\gamma(\boldsymbol{y}) + \int_{\Gamma_p} G(\boldsymbol{x},\boldsymbol{y}) f_z(\boldsymbol{y}) \, \mathrm{d}\gamma(\boldsymbol{y}) \\ &\qquad - \int_{\Gamma_\infty^R} \left(\frac{\partial G}{\partial y_2}(\boldsymbol{x},\boldsymbol{y}) + Z_\infty G(\boldsymbol{x},\boldsymbol{y}) \right) u(\boldsymbol{y}) \, \mathrm{d}\gamma(\boldsymbol{y}), \end{aligned} \tag{3.152}$$

where the integral on Γ_∞^R vanishes due the impedance boundary condition in (3.20). Therefore this term does not depend on R and has its support only on the bounded and perturbed portion Γ_p of the boundary.

In conclusion, when the limits $R \to \infty$ and $\varepsilon \to 0$ are taken in (3.142), then we obtain for $\boldsymbol{x} \in \Omega_e$ the integral representation formula

$$u(\boldsymbol{x}) = \int_{\Gamma_p} \left(\frac{\partial G}{\partial n_{\boldsymbol{y}}}(\boldsymbol{x},\boldsymbol{y}) - Z(\boldsymbol{y}) G(\boldsymbol{x},\boldsymbol{y}) \right) u(\boldsymbol{y}) \, \mathrm{d}\gamma(\boldsymbol{y}) + \int_{\Gamma_p} G(\boldsymbol{x},\boldsymbol{y}) f_z(\boldsymbol{y}) \, \mathrm{d}\gamma(\boldsymbol{y}), \tag{3.153}$$

which can be alternatively expressed as

$$u(\boldsymbol{x}) = \int_{\Gamma_p} \left(u(\boldsymbol{y}) \frac{\partial G}{\partial n_{\boldsymbol{y}}}(\boldsymbol{x},\boldsymbol{y}) - G(\boldsymbol{x},\boldsymbol{y}) \frac{\partial u}{\partial n}(\boldsymbol{y}) \right) \mathrm{d}\gamma(\boldsymbol{y}). \tag{3.154}$$

It is remarkable in this integral representation that the support of the integral, namely the curve Γ_p, is bounded. Let us denote the traces of the solution and of its normal derivative

on Γ_p respectively by

$$\mu = u|_{\Gamma_p} \qquad \text{and} \qquad \nu = \left.\frac{\partial u}{\partial n}\right|_{\Gamma_p}. \tag{3.155}$$

We can rewrite now (3.153) and (3.154) in terms of layer potentials as

$$u = \mathcal{D}(\mu) - \mathcal{S}(Z\mu) + \mathcal{S}(f_z) \qquad \text{in } \Omega_e, \tag{3.156}$$

$$u = \mathcal{D}(\mu) - \mathcal{S}(\nu) \qquad \text{in } \Omega_e, \tag{3.157}$$

where we define for $\boldsymbol{x} \in \Omega_e$ respectively the single and double layer potentials as

$$\mathcal{S}\nu(\boldsymbol{x}) = \int_{\Gamma_p} G(\boldsymbol{x}, \boldsymbol{y})\nu(\boldsymbol{y})\,\mathrm{d}\gamma(\boldsymbol{y}), \tag{3.158}$$

$$\mathcal{D}\mu(\boldsymbol{x}) = \int_{\Gamma_p} \frac{\partial G}{\partial n_{\boldsymbol{y}}}(\boldsymbol{x}, \boldsymbol{y})\mu(\boldsymbol{y})\,\mathrm{d}\gamma(\boldsymbol{y}). \tag{3.159}$$

We remark that from the impedance boundary condition (3.4) it is clear that

$$\nu = Z\mu - f_z. \tag{3.160}$$

3.6.2 Integral equation

To determine entirely the solution of the direct scattering problem (3.13) by means of its integral representation, we have to find values for the traces (3.155). This requires the development of an integral equation that allows to fix these values by incorporating the boundary data. For this purpose we place the source point $\boldsymbol{x}$ on the boundary Γ and apply the same procedure as before for the integral representation (3.153), treating differently in (3.142) only the integrals on S_ε. The integrals on S_R^+ still behave well and tend towards zero as $R \to \infty$. The Ball B_ε, though, is split in half by the boundary Γ, and the portion $\Omega_e \cap B_\varepsilon$ is asymptotically separated from its complement in B_ε by the tangent of the boundary if Γ is regular. If $\boldsymbol{x} \in \Gamma_+$, then the associated integrals on S_ε give rise to a term $-u(\boldsymbol{x})/2$ instead of just $-u(\boldsymbol{x})$ as before for the integral representation. Therefore we obtain for $\boldsymbol{x} \in \Gamma_+$ the boundary integral representation

$$\frac{u(\boldsymbol{x})}{2} = \int_{\Gamma_p} \left(\frac{\partial G}{\partial n_{\boldsymbol{y}}}(\boldsymbol{x}, \boldsymbol{y}) - Z(\boldsymbol{y})G(\boldsymbol{x}, \boldsymbol{y}) \right) u(\boldsymbol{y})\,\mathrm{d}\gamma(\boldsymbol{y}) + \int_{\Gamma_p} G(\boldsymbol{x}, \boldsymbol{y}) f_z(\boldsymbol{y})\,\mathrm{d}\gamma(\boldsymbol{y}). \tag{3.161}$$

On the contrary, if $\boldsymbol{x} \in \Gamma_0$, then the logarithmic behavior (3.98) contributes also to the singularity (3.97) of the Green's function and the integrals on S_ε give now rise to two terms $-u(\boldsymbol{x})/2$, i.e., on the whole to a term $-u(\boldsymbol{x})$. For $\boldsymbol{x} \in \Gamma_0$ the boundary integral representation is instead given by

$$u(\boldsymbol{x}) = \int_{\Gamma_p} \left(\frac{\partial G}{\partial n_{\boldsymbol{y}}}(\boldsymbol{x}, \boldsymbol{y}) - Z(\boldsymbol{y})G(\boldsymbol{x}, \boldsymbol{y}) \right) u(\boldsymbol{y})\,\mathrm{d}\gamma(\boldsymbol{y}) + \int_{\Gamma_p} G(\boldsymbol{x}, \boldsymbol{y}) f_z(\boldsymbol{y})\,\mathrm{d}\gamma(\boldsymbol{y}). \tag{3.162}$$

We must notice that in both cases, the integrands associated with the boundary Γ admit an integrable singularity at the point $\boldsymbol{x}$. In terms of boundary layer potentials, we can express these boundary integral representations as

$$\frac{u}{2} = D(\mu) - S(Z\mu) + S(f_z) \qquad \text{on } \Gamma_+, \tag{3.163}$$

$$u = D(\mu) - S(Z\mu) + S(f_z) \qquad \text{on } \Gamma_0, \tag{3.164}$$

where we consider, for $\boldsymbol{x} \in \Gamma$, the two boundary integral operators

$$S\nu(\boldsymbol{x}) = \int_{\Gamma_p} G(\boldsymbol{x}, \boldsymbol{y})\nu(\boldsymbol{y})\, \mathrm{d}\gamma(\boldsymbol{y}), \tag{3.165}$$

$$D\mu(\boldsymbol{x}) = \int_{\Gamma_p} \frac{\partial G}{\partial n_{\boldsymbol{y}}}(\boldsymbol{x}, \boldsymbol{y})\mu(\boldsymbol{y})\, \mathrm{d}\gamma(\boldsymbol{y}). \tag{3.166}$$

We can combine (3.163) and (3.164) into a single integral equation on Γ_p, namely

$$(1 + \mathcal{I}_0)\frac{\mu}{2} + S(Z\mu) - D(\mu) = S(f_z) \qquad \text{on } \Gamma_p, \tag{3.167}$$

where $\mathcal{I}_0$ denotes the characteristic or indicator function of the set Γ_0, i.e.,

$$\mathcal{I}_0(\boldsymbol{x}) = \begin{cases} 1 & \text{if } \boldsymbol{x} \in \Gamma_0, \\ 0 & \text{if } \boldsymbol{x} \notin \Gamma_0. \end{cases} \tag{3.168}$$

It is the solution μ on Γ_p of the integral equation (3.167) which finally allows to characterize the solution u in Ω_e of the direct scattering problem (3.13) through the integral representation formula (3.156). The trace of the solution u on the boundary Γ is then found simultaneously by means of the boundary integral representations (3.163) and (3.164). In particular, when $\boldsymbol{x} \in \Gamma_\infty$ and since $\Gamma_\infty \subset \Gamma_0$, therefore it holds that

$$u = D(\mu) - S(Z\mu) + S(f_z) \qquad \text{on } \Gamma_\infty. \tag{3.169}$$

3.7 Far field of the solution

The asymptotic behavior at infinity of the solution u of (3.13) is described by the far field. It is denoted by u^{ff} and is characterized by

$$u(\boldsymbol{x}) \sim u^{ff}(\boldsymbol{x}) \qquad \text{as } |\boldsymbol{x}| \to \infty. \tag{3.170}$$

Its expression can be deduced by replacing the far field of the Green's function G^{ff} and its derivatives in the integral representation formula (3.154), which yields

$$u^{ff}(\boldsymbol{x}) = \int_{\Gamma_p} \left(\frac{\partial G^{ff}}{\partial n_{\boldsymbol{y}}}(\boldsymbol{x}, \boldsymbol{y})\mu(\boldsymbol{y}) - G^{ff}(\boldsymbol{x}, \boldsymbol{y})\nu(\boldsymbol{y}) \right) \mathrm{d}\gamma(\boldsymbol{y}). \tag{3.171}$$

By replacing now (3.129) and the addition of (3.122) and (3.127) in (3.171), we obtain that

$$\begin{aligned} u^{ff}(\boldsymbol{x}) = \frac{e^{i\pi/4}}{\sqrt{8\pi k}} \frac{e^{ik|\boldsymbol{x}|}}{\sqrt{|\boldsymbol{x}|}} \int_{\Gamma_p} e^{-ik\hat{\boldsymbol{x}}\cdot\boldsymbol{y}} \Bigg(& ik\hat{\boldsymbol{x}} \cdot \boldsymbol{n}_{\boldsymbol{y}}\, \mu(\boldsymbol{y}) + \nu(\boldsymbol{y}) \\ & - \frac{Z_\infty - ik\sin\theta}{Z_\infty + ik\sin\theta}\, e^{2iky_2\sin\theta} \left(ik \begin{bmatrix} \cos\theta \\ -\sin\theta \end{bmatrix} \cdot \boldsymbol{n}_{\boldsymbol{y}}\, \mu(\boldsymbol{y}) + \nu(\boldsymbol{y}) \right) \Bigg) \mathrm{d}\gamma(\boldsymbol{y}) \\ - \frac{Z_\infty}{\xi_p}\, e^{-Z_\infty x_2} e^{iZ_\infty |x_1|} \int_{\Gamma_p} e^{-Z_\infty y_2} e^{-iZ_\infty y_1 \operatorname{sign} x_1} & \left(\begin{bmatrix} \xi_p \operatorname{sign} x_1 \\ -iZ_\infty \end{bmatrix} \cdot \boldsymbol{n}_{\boldsymbol{y}}\, \mu(\boldsymbol{y}) - i\nu(\boldsymbol{y}) \right) \mathrm{d}\gamma(\boldsymbol{y}). \end{aligned} \tag{3.172}$$

The asymptotic behavior of the solution u at infinity, as $|\boldsymbol{x}| \to \infty$, is therefore given by

$$u(\boldsymbol{x}) = \frac{e^{ik|\boldsymbol{x}|}}{\sqrt{|\boldsymbol{x}|}} \left\{ u_\infty^V(\hat{\boldsymbol{x}}) + \mathcal{O}\left(\frac{1}{|\boldsymbol{x}|}\right) \right\} + e^{-Z_\infty x_2} e^{i\xi_p |x_1|} \left\{ u_\infty^S(\hat{x}_s) + \mathcal{O}\left(\frac{1}{|x_1|}\right) \right\}, \quad (3.173)$$

where $\hat{x}_s = \operatorname{sign} x_1$ and where we decompose $\boldsymbol{x} = |\boldsymbol{x}|\, \hat{\boldsymbol{x}}$, being $\hat{\boldsymbol{x}} = (\cos\theta,\, \sin\theta)$ a vector of the unit circle. The far-field pattern of the volume waves is given by

$$u_\infty^V(\hat{\boldsymbol{x}}) = \frac{e^{i\pi/4}}{\sqrt{8\pi k}} \int_{\Gamma_p} e^{-ik\hat{\boldsymbol{x}}\cdot\boldsymbol{y}} \Bigg(ik\hat{\boldsymbol{x}} \cdot \boldsymbol{n_y}\, \mu(\boldsymbol{y}) + \nu(\boldsymbol{y}) \\ - \frac{Z_\infty - ik\sin\theta}{Z_\infty + ik\sin\theta}\, e^{2iky_2 \sin\theta} \left(ik \begin{bmatrix} \cos\theta \\ -\sin\theta \end{bmatrix} \cdot \boldsymbol{n_y}\, \mu(\boldsymbol{y}) + \nu(\boldsymbol{y}) \right) \Bigg) \mathrm{d}\gamma(\boldsymbol{y}), \quad (3.174)$$

whereas the far-field pattern for the surface waves adopts the form

$$u_\infty^S(\hat{x}_s) = -\frac{Z_\infty}{\xi_p} \int_{\Gamma_p} e^{-Z_\infty y_2} e^{-iZ_\infty y_1 \operatorname{sign} x_1} \left(\begin{bmatrix} \xi_p \operatorname{sign} x_1 \\ -iZ_\infty \end{bmatrix} \cdot \boldsymbol{n_y}\, \mu(\boldsymbol{y}) - i\nu(\boldsymbol{y}) \right) \mathrm{d}\gamma(\boldsymbol{y}). \quad (3.175)$$

Both far-field patterns can be expressed in decibels (dB) respectively by means of the scattering cross sections

$$Q_s^V(\hat{\boldsymbol{x}}) \ \ [\mathrm{dB}] = 20 \log_{10}\left(\frac{|u_\infty^V(\hat{\boldsymbol{x}})|}{|u_0^V|} \right), \quad (3.176)$$

$$Q_s^S(\hat{x}_s) \ \ [\mathrm{dB}] = 20 \log_{10}\left(\frac{|u_\infty^S(\hat{x}_s)|}{|u_0^S|} \right), \quad (3.177)$$

where the reference levels u_0^V and u_0^S are taken such that $|u_0^V| = |u_0^S| = 1$ if the incident field is given either by a volume wave of the form (3.16) or by a surface wave of the form (3.19).

We remark that the far-field behavior (3.173) of the solution is in accordance with the radiation condition (3.6), which justifies its choice.

3.8 Existence and uniqueness

3.8.1 Function spaces

To state a precise mathematical formulation of the herein treated problems, we have to define properly the involved function spaces. Since the considered domains and boundaries are unbounded, we need to work with weighted Sobolev spaces, as in Durán, Muga & Nédélec (2005*a*, 2006). We consider the classic weight functions

$$\varrho = \sqrt{1 + r^2} \qquad \text{and} \qquad \log \varrho = \ln(2 + r^2), \quad (3.178)$$

where $r = |\boldsymbol{x}|$. We define the domains

$$\Omega_e^1 = \left\{ \boldsymbol{x} \in \Omega_e : \ x_2 > \frac{1}{2Z_\infty} \ln\left(1 + \frac{8\pi k Z_\infty^2}{Z_\infty^2 + k^2}\, r \right) \right\}, \quad (3.179)$$

$$\Omega_e^2 = \left\{ \boldsymbol{x} \in \Omega_e : \ x_2 < \frac{1}{2Z_\infty} \ln\left(1 + \frac{8\pi k Z_\infty^2}{Z_\infty^2 + k^2}\, r \right) \right\}. \quad (3.180)$$

It holds that the solution of the direct scattering problem (3.13) is contained in the weighted Sobolev space

$$W^1(\Omega_e) = \Bigg\{ v : \frac{v}{\varrho \log \varrho} \in L^2(\Omega_e),\ \frac{\nabla v}{\varrho \log \varrho} \in L^2(\Omega_e)^2,\ \frac{v}{\sqrt{\varrho}} \in L^2(\Omega_e^1),$$
$$\frac{\partial v}{\partial r} - ikv \in L^2(\Omega_e^1),\ \frac{v}{\log \varrho} \in L^2(\Omega_e^2),\ \frac{1}{\log \varrho}\left(\frac{\partial v}{\partial r} - i\xi_p v\right) \in L^2(\Omega_e^2) \Bigg\}, \quad (3.181)$$

where $\xi_p = \sqrt{Z_\infty^2 + k^2}$. With the appropriate norm, the space $W^1(\Omega_e)$ becomes also a Hilbert space. We have likewise the inclusion $W^1(\Omega_e) \subset H^1_{\text{loc}}(\Omega_e)$, i.e., the functions of these two spaces differ only by their behavior at infinity.

Since we are dealing with Sobolev spaces, even a strong Lipschitz boundary $\Gamma \in C^{0,1}$ is admissible. The fact that this boundary Γ is also unbounded implies that we have to use weighted trace spaces like in Amrouche (2002). For this purpose, we consider the space

$$W^{1/2}(\Gamma) = \left\{ v : \frac{v}{\sqrt{\varrho} \log \varrho} \in H^{1/2}(\Gamma) \right\}. \quad (3.182)$$

Its dual space $W^{-1/2}(\Gamma)$ is defined via W^0-duality, i.e., considering the pivot space

$$W^0(\Gamma) = \left\{ v : \frac{v}{\sqrt{\varrho} \log \varrho} \in L^2(\Gamma) \right\}. \quad (3.183)$$

Analogously as for the trace theorem (A.531), if $v \in W^1(\Omega_e)$ then the trace of v fulfills

$$\gamma_0 v = v|_\Gamma \in W^{1/2}(\Gamma). \quad (3.184)$$

Moreover, the trace of the normal derivative can be also defined, and it holds that

$$\gamma_1 v = \frac{\partial v}{\partial n}|_\Gamma \in W^{-1/2}(\Gamma). \quad (3.185)$$

We remark further that the restriction of the trace of v to Γ_p is such that

$$\gamma_0 v|_{\Gamma_p} = v|_{\Gamma_p} \in H^{1/2}(\Gamma_p), \quad (3.186)$$

$$\gamma_1 v|_{\Gamma_p} = \frac{\partial v}{\partial n}|_{\Gamma_p} \in H^{-1/2}(\Gamma_p), \quad (3.187)$$

and its restriction to Γ_∞ yields

$$\gamma_0 v|_{\Gamma_\infty} = v|_{\Gamma_\infty} \in W^{1/2}(\Gamma_\infty), \quad (3.188)$$

$$\gamma_1 v|_{\Gamma_\infty} = \frac{\partial v}{\partial n}|_{\Gamma_\infty} \in W^{-1/2}(\Gamma_\infty). \quad (3.189)$$

3.8.2 Application to the integral equation

The existence and uniqueness of the solution for the direct scattering problem (3.13), due the integral representation formula (3.156), can be characterized by using the integral equation (3.167). For this purpose and in accordance with the considered function spaces, we take $\mu \in H^{1/2}(\Gamma_p)$ and $\nu \in H^{-1/2}(\Gamma_p)$. Furthermore, we consider that $Z \in L^\infty(\Gamma_p)$ and that $f_z \in H^{-1/2}(\Gamma_p)$, even though strictly speaking $f_z \in \widetilde{H}^{-1/2}(\Gamma_p)$.

It holds that the single and double layer potentials defined respectively in (3.158) and (3.159) are linear and continuous integral operators such that

$$\mathcal{S} : H^{-1/2}(\Gamma_p) \longrightarrow W^1(\Omega_e) \qquad \text{and} \qquad \mathcal{D} : H^{1/2}(\Gamma_p) \longrightarrow W^1(\Omega_e). \tag{3.190}$$

The boundary integral operators (3.165) and (3.166) are also linear and continuous applications, and they are such that

$$S : H^{-1/2}(\Gamma_p) \longrightarrow W^{1/2}(\Gamma) \qquad \text{and} \qquad D : H^{1/2}(\Gamma_p) \longrightarrow W^{1/2}(\Gamma). \tag{3.191}$$

When we restrict them to Γ_p, then it holds that

$$S|_{\Gamma_p} : H^{-1/2}(\Gamma_p) \longrightarrow H^{1/2}(\Gamma_p) \qquad \text{and} \qquad D|_{\Gamma_p} : H^{1/2}(\Gamma_p) \longrightarrow H^{1/2}(\Gamma_p). \tag{3.192}$$

Let us consider the integral equation (3.167), which is given in terms of boundary layer potentials, for $\mu \in H^{1/2}(\Gamma_p)$, by

$$(1 + \mathcal{I}_0)\frac{\mu}{2} + S(Z\mu) - D(\mu) = S(f_z) \qquad \text{in } \ H^{1/2}(\Gamma_p). \tag{3.193}$$

Due the imbedding properties of Sobolev spaces and in the same way as for the half-plane impedance Laplace problem, it holds that the left-hand side of the integral equation corresponds to an identity and two compact operators, and thus Fredholm's alternative holds.

Since the Fredholm alternative applies to the integral equation, therefore it applies also to the direct scattering problem (3.13) due the integral representation formula. The existence of the scattering problem's solution is thus determined by its uniqueness, and the wave numbers $k \in \mathbb{C}$ and impedances $Z \in \mathbb{C}$ for which the uniqueness is lost constitute a countable set, which we call respectively wave number spectrum and impedance spectrum of the scattering problem and denote it by σ_k and σ_Z. The spectrum σ_k considers a fixed Z and, conversely, the spectrum σ_Z considers a fixed k. The existence and uniqueness of the solution is therefore ensured almost everywhere. The same holds obviously for the solution of the integral equation, whose wave number spectrum and impedance spectrum we denote respectively by ς_k and ς_Z. Since each integral equation is derived from the scattering problem, it holds that $\sigma_k \subset \varsigma_k$ and $\sigma_Z \subset \varsigma_Z$. The converse, though, is not necessarily true. In any way, the sets $\varsigma_k \setminus \sigma_k$ and $\varsigma_Z \setminus \sigma_Z$ are at most countable.

In conclusion, the scattering problem (3.13) admits a unique solution u if $k \notin \sigma_k$ and $Z \notin \sigma_Z$, and the integral equation (3.167) admits in the same way a unique solution μ if $k \notin \varsigma_k$ and $Z \notin \varsigma_Z$.

3.9 Dissipative problem

The dissipative problem considers waves that dissipate their energy as they propagate and are modeled by considering a complex wave number or a complex impedance. The use of a complex wave number $k \in \mathbb{C}$ whose imaginary part is strictly positive, i.e., such that $\mathfrak{Im}\{k\} > 0$, ensures an exponential decrease at infinity for both the volume and the surface waves. On the other hand, the use of a complex impedance $Z_\infty \in \mathbb{C}$ with a strictly positive imaginary part, i.e., $\mathfrak{Im}\{Z_\infty\} > 0$, ensures only an exponential decrease at infinity for the surface waves. In the first case, when considering a complex wave number k, and

due the dissipative nature of the medium, it is no longer suited to take progressive plane volume waves in the form of (3.16) and (3.17) respectively as the incident field u_I and the reflected field u_R. In both cases, likewise, it is no longer suited to take progressive plane surface waves in the form of (3.19) as the incident field u_I. Instead, we have to take a wave source at a finite distance from the perturbation. For example, we can consider a point source located at $\boldsymbol{z} \in \Omega_e$, in which case we have only an incident field, which is given, up to a multiplicative constant, by

$$u_I(\boldsymbol{x}) = G(\boldsymbol{x}, \boldsymbol{z}), \tag{3.194}$$

where G denotes the Green's function (3.93). This incident field u_I satisfies the Helmholtz equation with a source term in the right-hand side, namely

$$\Delta u_I + k^2 u_I = \delta_{\boldsymbol{z}} \qquad \text{in } \mathcal{D}'(\Omega_e), \tag{3.195}$$

which holds also for the total field u_T but not for the scattered field u, in which case the Helmholtz equation remains homogeneous. For a general source distribution g_s, whose support is contained in Ω_e, the incident field can be expressed by

$$u_I(\boldsymbol{x}) = G(\boldsymbol{x}, \boldsymbol{z}) * g_s(\boldsymbol{z}) = \int_{\Omega_e} G(\boldsymbol{x}, \boldsymbol{z})\, g_s(\boldsymbol{z})\, \mathrm{d}\boldsymbol{z}. \tag{3.196}$$

This incident field u_I satisfies now

$$\Delta u_I + k^2 u_I = g_s \qquad \text{in } \mathcal{D}'(\Omega_e), \tag{3.197}$$

which holds again also for the total field u_T but not for the scattered field u.

It is not difficult to see that all the performed developments for the non-dissipative case are still valid when considering dissipation. The only difference is that now either a complex wave number k such that $\mathfrak{Im}\{k\} > 0$, or a complex impedance Z_∞ such that $\mathfrak{Im}\{Z_\infty\} > 0$, or both, have to be taken everywhere into account.

3.10 Variational formulation

To solve the integral equation we convert it to its variational or weak formulation, i.e., we solve it with respect to a certain test function in a bilinear (or sesquilinear) form. Basically, the integral equation is multiplied by the (conjugated) test function and then the equation is integrated over the boundary of the domain. The test function is taken in the same function space as the solution of the integral equation.

The variational formulation for the integral equation (3.193) searches $\mu \in H^{1/2}(\Gamma_p)$ such that $\forall \varphi \in H^{1/2}(\Gamma_p)$ we have that

$$\Big\langle (1 + \mathcal{I}_0)\frac{\mu}{2} + S(Z\mu) - D(\mu), \varphi \Big\rangle = \big\langle S(f_z), \varphi \big\rangle. \tag{3.198}$$

3.11 Numerical discretization

3.11.1 Discretized function spaces

The scattering problem (3.13) is solved numerically with the boundary element method by employing a Galerkin scheme on the variational formulation of the integral equation. We use on the boundary curve Γ_p Lagrange finite elements of type $\mathbb{P}_1$. As shown in Figure 3.9, the curve Γ_p is approximated by the discretized curve Γ_p^h, composed by I rectilinear segments T_j, sequentially ordered from left to right for $1 \leq j \leq I$, such that their length $|T_j|$ is less or equal than h, and with their endpoints on top of Γ_p.

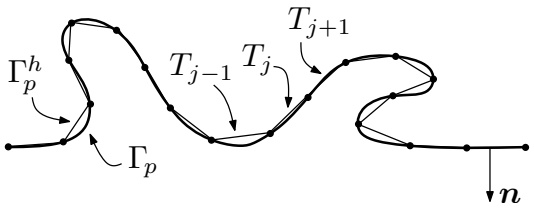

FIGURE 3.9. Curve Γ_p^h, discretization of Γ_p.

The function space $H^{1/2}(\Gamma_p)$ is approximated using the conformal space of continuous piecewise linear polynomials with complex coefficients

$$Q_h = \big\{\varphi_h \in C^0(\Gamma_p^h) \,:\, \varphi_h|_{T_j} \in \mathbb{P}_1(\mathbb{C}),\;\; 1 \leq j \leq I\big\}. \tag{3.199}$$

The space Q_h has a finite dimension $(I+1)$, and we describe it using the standard base functions for finite elements of type $\mathbb{P}_1$, denoted by $\{\chi_j\}_{j=1}^{I+1}$ and expressed as

$$\chi_j(\boldsymbol{x}) = \begin{cases} \dfrac{|\boldsymbol{x} - \boldsymbol{r}_{j-1}|}{|T_{j-1}|} & \text{if } \; \boldsymbol{x} \in T_{j-1}, \\ \dfrac{|\boldsymbol{r}_{j+1} - \boldsymbol{x}|}{|T_j|} & \text{if } \; \boldsymbol{x} \in T_j, \\ 0 & \text{if } \; \boldsymbol{x} \notin T_{j-1} \cup T_j, \end{cases} \tag{3.200}$$

where segment T_{j-1} has as endpoints $\boldsymbol{r}_{j-1}$ and $\boldsymbol{r}_j$, while the endpoints of segment T_j are given by $\boldsymbol{r}_j$ and $\boldsymbol{r}_{j+1}$.

In virtue of this discretization, any function $\varphi_h \in Q_h$ can be expressed as a linear combination of the elements of the base, namely

$$\varphi_h(\boldsymbol{x}) = \sum_{j=1}^{I+1} \varphi_j \, \chi_j(\boldsymbol{x}) \qquad \text{for } \; \boldsymbol{x} \in \Gamma_p^h, \tag{3.201}$$

where $\varphi_j \in \mathbb{C}$ for $1 \leq j \leq I+1$. The solution $\mu \in H^{1/2}(\Gamma_p)$ of the variational formulation (3.198) can be therefore approximated by

$$\mu_h(\boldsymbol{x}) = \sum_{j=1}^{I+1} \mu_j \, \chi_j(\boldsymbol{x}) \qquad \text{for } \; \boldsymbol{x} \in \Gamma_p^h, \tag{3.202}$$

where $\mu_j \in \mathbb{C}$ for $1 \leq j \leq I+1$. The function f_z can be also approximated by

$$f_z^h(\boldsymbol{x}) = \sum_{j=1}^{I+1} f_j \, \chi_j(\boldsymbol{x}) \qquad \text{for } \boldsymbol{x} \in \Gamma_p^h, \quad \text{with } f_j = f_z(\boldsymbol{r}_j). \tag{3.203}$$

3.11.2 Discretized integral equation

To see how the boundary element method operates, we apply it to the variational formulation (3.198). We characterize all the discrete approximations by the index h, including also the impedance and the boundary layer potentials. The numerical approximation of (3.198) leads to the discretized problem that searches $\mu_h \in Q_h$ such that $\forall \varphi_h \in Q_h$

$$\Big\langle (1 + \mathcal{I}_0^h)\frac{\mu_h}{2} + S_h(Z_h\mu_h) - D_h(\mu_h), \varphi_h \Big\rangle = \big\langle S_h(f_z^h), \varphi_h \big\rangle. \tag{3.204}$$

Considering the decomposition of μ_h in terms of the base $\{\chi_j\}$ and taking as test functions the same base functions, $\varphi_h = \chi_i$ for $1 \leq i \leq I+1$, yields the discrete linear system

$$\sum_{j=1}^{I+1} \mu_j \left(\frac{1}{2}\big\langle (1 + \mathcal{I}_0^h)\chi_j, \chi_i \big\rangle + \langle S_h(Z_h\chi_j), \chi_i \rangle - \langle D_h(\chi_j), \chi_i \rangle \right) = \sum_{j=1}^{I+1} f_j \, \langle S_h(\chi_j), \chi_i \rangle. \tag{3.205}$$

This constitutes a system of linear equations that can be expressed as a linear matrix system:

$$\begin{cases} \text{Find } \boldsymbol{\mu} \in \mathbb{C}^{I+1} \text{ such that} \\ \boldsymbol{M}\boldsymbol{\mu} = \boldsymbol{b}. \end{cases} \tag{3.206}$$

The elements m_{ij} of the matrix $\boldsymbol{M}$ are given, for $1 \leq i, j \leq I+1$, by

$$m_{ij} = \frac{1}{2}\big\langle (1 + \mathcal{I}_0^h)\chi_j, \chi_i \big\rangle + \langle S_h(Z_h\chi_j), \chi_i \rangle - \langle D_h(\chi_j), \chi_i \rangle, \tag{3.207}$$

and the elements b_i of the vector $\boldsymbol{b}$ by

$$b_i = \big\langle S_h(f_z^h), \chi_i \big\rangle = \sum_{j=1}^{I+1} f_j \, \langle S_h(\chi_j), \chi_i \rangle \qquad \text{for } 1 \leq i \leq I+1. \tag{3.208}$$

The discretized solution u_h, which approximates u, is finally obtained by discretizing the integral representation formula (3.156) according to

$$u_h = \mathcal{D}_h(\mu_h) - \mathcal{S}_h(Z_h\mu_h) + \mathcal{S}_h(f_z^h), \tag{3.209}$$

which, more specifically, can be expressed as

$$u_h = \sum_{j=1}^{I+1} \mu_j \big(\mathcal{D}_h(\chi_j) - \mathcal{S}_h(Z_h\chi_j) \big) + \sum_{j=1}^{I+1} f_j \, \mathcal{S}_h(\chi_j). \tag{3.210}$$

We remark that the resulting matrix $\boldsymbol{M}$ is in general complex, full, non-symmetric, and with dimensions $(I+1) \times (I+1)$. The right-hand side vector $\boldsymbol{b}$ is complex and of size $I+1$. The boundary element calculations required to compute numerically the elements of $\boldsymbol{M}$ and $\boldsymbol{b}$ have to be performed carefully, since the integrals that appear become singular when the involved segments are adjacent or coincident, due the singularity of the

Green's function at its source point. On Γ_0, the singularity of the image source point has to be taken additionally into account for these calculations.

3.12 Boundary element calculations

The boundary element calculations build the elements of the matrix $\boldsymbol{M}$ resulting from the discretization of the integral equation, i.e., from (3.206). They permit thus to compute numerically expressions like (3.207). To evaluate the appearing singular integrals, we adapt the semi-numerical methods described in the report of Bendali & Devys (1986).

We use the same notation as in Section B.12, and the required boundary element integrals, for $a, b \in \{1, 2\}$, are again

$$ZA_{a,b} = \int_K \int_L \left(\frac{s}{|K|}\right)^a \left(\frac{t}{|L|}\right)^b G(\boldsymbol{x}, \boldsymbol{y}) \, \mathrm{d}L(\boldsymbol{y}) \, \mathrm{d}K(\boldsymbol{x}), \tag{3.211}$$

$$ZB_{a,b} = \int_K \int_L \left(\frac{s}{|K|}\right)^a \left(\frac{t}{|L|}\right)^b \frac{\partial G}{\partial n_{\boldsymbol{y}}}(\boldsymbol{x}, \boldsymbol{y}) \, \mathrm{d}L(\boldsymbol{y}) \, \mathrm{d}K(\boldsymbol{x}). \tag{3.212}$$

All the integrals that stem from the numerical discretization can be expressed in terms of these two basic boundary element integrals. The impedance is again discretized as a piecewise constant function Z_h, which on each segment T_j adopts a constant value $Z_j \in \mathbb{C}$. The integrals of interest are the same as for the full-plane impedance Helmholtz problem and we consider furthermore that

$$\left\langle (1 + \mathcal{I}_0^h)\chi_j, \chi_i \right\rangle = \begin{cases} \langle \chi_j, \chi_i \rangle & \text{if } \boldsymbol{r}_j \in \Gamma_+, \\ 2 \langle \chi_j, \chi_i \rangle & \text{if } \boldsymbol{r}_j \in \Gamma_0. \end{cases} \tag{3.213}$$

To compute the boundary element integrals (3.211) and (3.212), we can easily isolate the singular part (3.97) of the Green's function (3.93), which corresponds in fact to the Green's function of the Laplace equation in the full-plane, and therefore the associated integrals are computed in the same way. The same applies also for its normal derivative. In the case when the segments K and L are are close enough, e.g., adjacent or coincident, and when $L \in \Gamma_0^h$ or $K \in \Gamma_0^h$, being Γ_0^h the approximation of Γ_0, we have to consider additionally the singular behavior (3.98), which is linked with the presence of the impedance half-plane. This behavior can be straightforwardly evaluated by replacing $\boldsymbol{x}$ by $\bar{\boldsymbol{x}}$ in formulae (B.340) to (B.343), i.e., by computing the quantities $ZF_b(\bar{\boldsymbol{x}})$ and $ZG_b(\bar{\boldsymbol{x}})$ with the corresponding adjustment of the notation. Otherwise, if the segments are not close enough and for the non-singular part of the Green's function, a two-point Gauss quadrature formula is used. All the other computations are performed in the same manner as in Section B.12 for the full-plane Laplace equation.

3.13 Benchmark problem

As benchmark problem we consider the particular case when the domain $\Omega_e \subset \mathbb{R}^2_+$ is taken as the exterior of a half-circle of radius $R > 0$ that is centered at the origin, as shown

in Figure 3.10. We decompose the boundary of Ω_e as $\Gamma = \Gamma_p \cup \Gamma_\infty$, where Γ_p corresponds to the upper half-circle, whereas Γ_∞ denotes the remaining unperturbed portion of the half-plane's boundary which lies outside the half-circle and which extends towards infinity on both sides. The unit normal $\boldsymbol{n}$ is taken outwardly oriented of Ω_e, e.g., $\boldsymbol{n} = -\boldsymbol{r}$ on Γ_p.

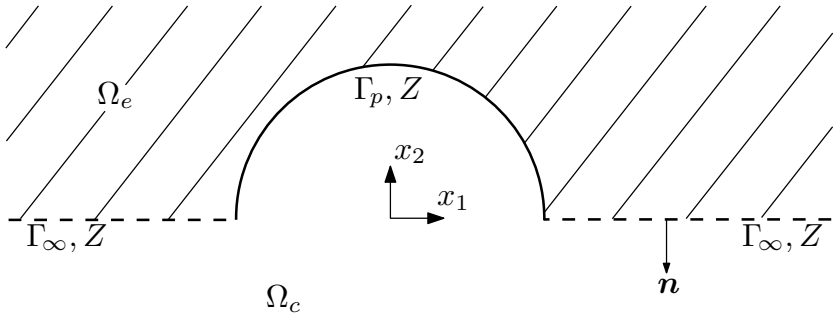

FIGURE 3.10. Exterior of the half-circle.

The benchmark problem is then stated as

$$\begin{cases} \text{Find } u : \Omega_e \to \mathbb{C} \text{ such that} \\ \Delta u + k^2 u = 0 \qquad \text{in } \Omega_e, \\ -\dfrac{\partial u}{\partial n} + Zu = f_z \qquad \text{on } \Gamma, \\ \text{+ Outgoing radiation condition as } |\boldsymbol{x}| \to \infty, \end{cases} \tag{3.214}$$

where we consider a wave number $k \in \mathbb{C}$, a constant impedance $Z \in \mathbb{C}$ throughout Γ, and where the radiation condition is as usual given by (3.6). As incident field u_I we consider the same Green's function, namely

$$u_I(\boldsymbol{x}) = G(\boldsymbol{x}, \boldsymbol{z}), \tag{3.215}$$

where $\boldsymbol{z} \in \Omega_c$ denotes the source point of our incident field. The impedance data function f_z is hence given by

$$f_z(\boldsymbol{x}) = \frac{\partial G}{\partial n_{\boldsymbol{x}}}(\boldsymbol{x}, \boldsymbol{z}) - ZG(\boldsymbol{x}, \boldsymbol{z}), \tag{3.216}$$

and its support is contained in Γ_p. The analytic solution for the benchmark problem (3.214) is then clearly given by

$$u(\boldsymbol{x}) = -G(\boldsymbol{x}, \boldsymbol{z}). \tag{3.217}$$

The goal is to retrieve this solution numerically with the integral equation techniques and the boundary element method described throughout this chapter.

For the computational implementation and the numerical resolution of the benchmark problem, we consider integral equation (3.167). The linear system (3.206) resulting from the discretization (3.204) of its variational formulation (3.198) is solved computationally with finite boundary elements of type $\mathbb{P}_1$ by using subroutines programmed in Fortran 90,

by generating the mesh Γ_p^h of the boundary with the free software Gmsh 2.4, and by representing graphically the results in Matlab 7.5 (R2007b).

We consider a radius $R = 1$, a wave number $k = 3$, a constant impedance $Z = 5$, and for the incident field a source point $\boldsymbol{z} = (0, 0)$. The discretized perturbed boundary curve Γ_p^h has $I = 120$ segments and a discretization step $h = 0.02618$, being

$$h = \max_{1 \leq j \leq I} |T_j|. \tag{3.218}$$

We observe that $h \approx \pi / I$.

The numerically calculated trace of the solution μ_h of the benchmark problem, which was computed by using the boundary element method, is depicted in Figure 3.11. In the same manner, the numerical solution u_h is illustrated in Figures 3.12 and 3.13. It can be observed that the numerical solution is quite close to the exact one.

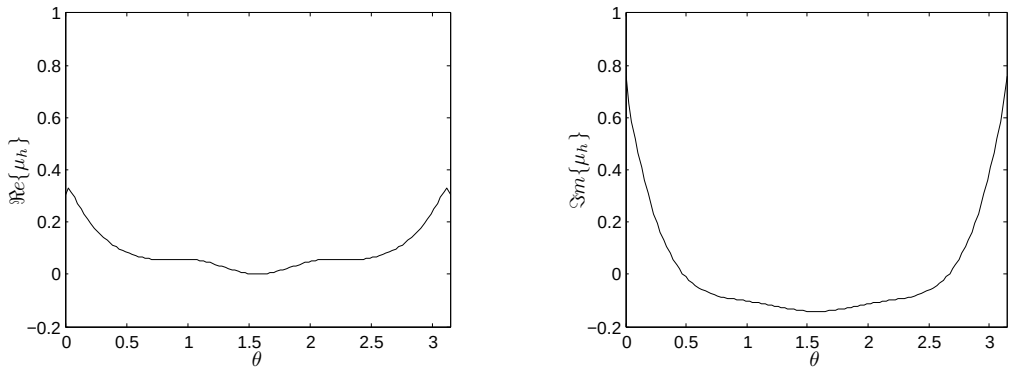

(a) Real part (b) Imaginary part

FIGURE 3.11. Numerically computed trace of the solution μ_h.

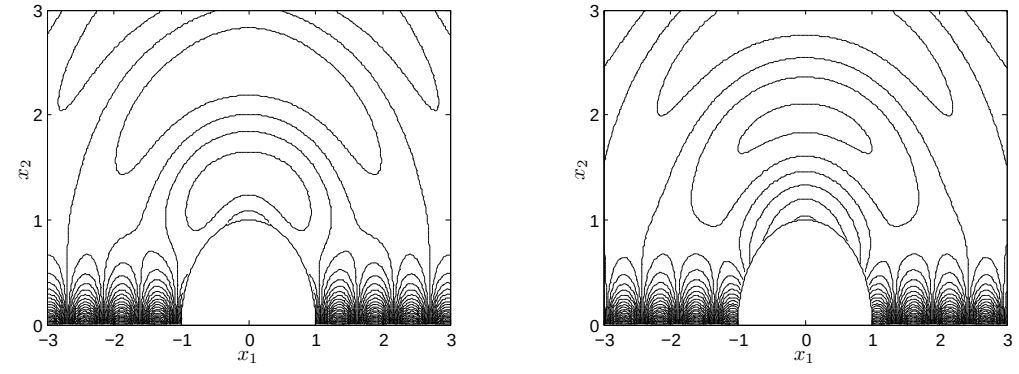

(a) Real part (b) Imaginary part

FIGURE 3.12. Contour plot of the numerically computed solution u_h.

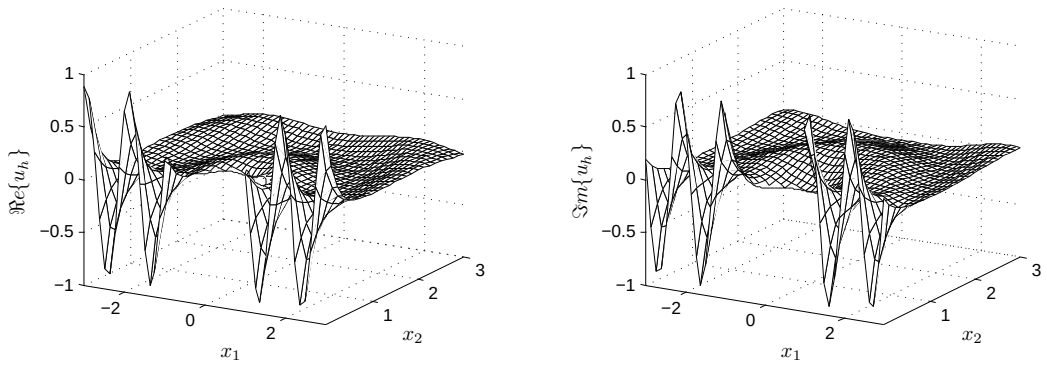

(a) Real part (b) Imaginary part

FIGURE 3.13. Oblique view of the numerically computed solution u_h.

Likewise as in (B.368), we define the relative error of the trace of the solution as

$$E_2(h, \Gamma_p^h) = \frac{\|\Pi_h \mu - \mu_h\|_{L^2(\Gamma_p^h)}}{\|\Pi_h \mu\|_{L^2(\Gamma_p^h)}}, \tag{3.219}$$

where $\Pi_h \mu$ denotes the Lagrange interpolating function of the exact solution's trace μ, i.e.,

$$\Pi_h \mu(\boldsymbol{x}) = \sum_{j=1}^{I+1} \mu(\boldsymbol{r}_j)\, \chi_j(\boldsymbol{x}) \quad \text{and} \quad \mu_h(\boldsymbol{x}) = \sum_{j=1}^{I+1} \mu_j\, \chi_j(\boldsymbol{x}) \quad \text{for } \boldsymbol{x} \in \Gamma_p^h. \tag{3.220}$$

In our case, for a step $h = 0.02618$, we obtained a relative error of $E_2(h, \Gamma_p^h) = 0.08631$.

As in (B.372), we define the relative error of the solution as

$$E_\infty(h, \Omega_L) = \frac{\|u - u_h\|_{L^\infty(\Omega_L)}}{\|u\|_{L^\infty(\Omega_L)}}, \tag{3.221}$$

being $\Omega_L = \{\boldsymbol{x} \in \Omega_e : \|\boldsymbol{x}\|_\infty < L\}$ for $L > 0$. We consider $L = 3$ and describe Ω_L by a triangular finite element mesh of refinement h near the boundary. For $h = 0.02618$, the relative error that we obtained for the solution was $E_\infty(h, \Omega_L) = 0.06178$.

The results for different mesh refinements, i.e., for different numbers of segments I and discretization steps h, are listed in Table 3.1. These results are illustrated graphically in Figure 3.14. It can be observed that the relative errors are approximately of order h for bigger values of h.

TABLE 3.1. Relative errors for different mesh refinements.

I	h	$E_2(h, \Gamma_p^h)$	$E_\infty(h, \Omega_L)$
12	0.2611	$8.483 \cdot 10^{-1}$	$7.702 \cdot 10^{-1}$
40	0.07852	$2.843 \cdot 10^{-1}$	$1.899 \cdot 10^{-1}$
80	0.03927	$1.316 \cdot 10^{-1}$	$9.362 \cdot 10^{-2}$
120	0.02618	$8.631 \cdot 10^{-2}$	$6.178 \cdot 10^{-2}$
240	0.01309	$5.076 \cdot 10^{-2}$	$3.177 \cdot 10^{-2}$
500	0.006283	$4.587 \cdot 10^{-2}$	$2.804 \cdot 10^{-2}$
1000	0.003142	$4.873 \cdot 10^{-2}$	$2.695 \cdot 10^{-2}$

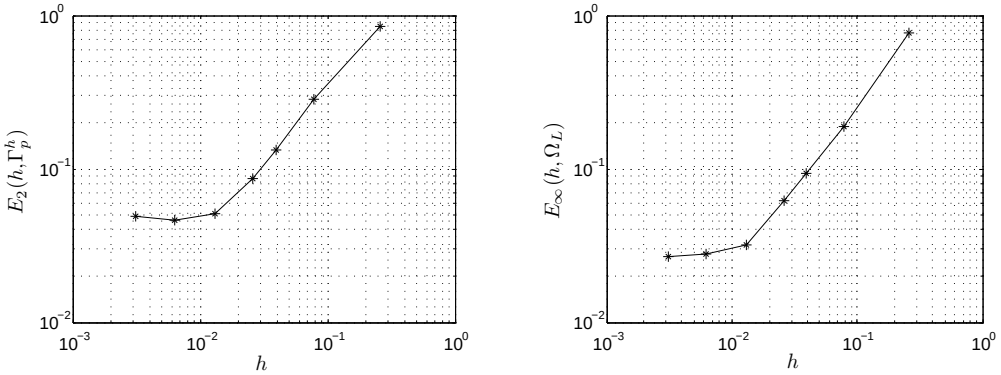

(a) Relative error $E_2(h, \Gamma_p^h)$ (b) Relative error $E_\infty(h, \Omega_L)$

FIGURE 3.14. Logarithmic plots of the relative errors versus the discretization step.